Precambrian Research 269 (2015) 90–106

Contents lists available at ScienceDirect

Precambrian Research

journal homepage: www.elsevier.com/locate/precamres

New paleomagnetic results from the Huaibei Group and Neoproterozoic mafic sills in the North China Craton and their paleogeographic implications

Xingmei Fu[a], Shihong Zhang[a,*], Haiyan Li[a,b], Jikai Ding[a], Huaikun Li[c], Tianshui Yang[a], Huaichun Wu[a], Haifan Yuan[c], Jing Lv[a]

[a] State Key Laboratory of Biogeology and Environmental Geology, China University of Geosciences, Beijing 100083, China
[b] Institute of Earth Sciences, China University of Geosciences, Beijing 100083, China
[c] Tianjin Institute of Geology and Mineral Resources, Tianjin 300170, China

ARTICLE INFO

Article history:
Received 18 February 2015
Received in revised form 27 July 2015
Accepted 6 August 2015
Available online 17 August 2015

Keywords:
Paleomagnetism
Neoproterozoic sills
Huaibei Group
North China
Rodinia

ABSTRACT

New paleomagnetic pole positions are obtained from the Neoproterozoic sills and carbonate rocks of the Huaibei Group in the northern Jiangsu and Anhui Provinces (Xuhuai region), North China. A total of 240 samples are used in statistics after stepwise thermal demagnetization and principal component analysis, including 85 samples from three ~890 Ma mafic sills, 27 samples from the ~890-Ma-sill-baked rocks of the Wangshan Formation (Fm), 50 samples from unbaked rocks of the Wangshan Fm, 60 samples from unbaked rocks of the Jiayuan Fm and 18 samples from a ~925 Ma mafic sill. For most of these samples, after removing a low unblocking temperature component (LTC) of viscous magnetic remanence acquired in recent geomagnetic field, high unblocking temperature components (HTCs), likely carried by magnetite for the sill and unbaked carbonate samples and by partly oxidized magnetite for baked carbonate samples, were isolated. The HTCs of the ~890 Ma sills passed a reversal test, a fold test, and a baked contact test. It is interpreted as a primary remanence, defining a key pole ($Q = 7$) at 52.6°N, 330.0°E ($A_{95} = 5.3°$) for the North China Craton (NCC). The HTCs of the unbaked carbonate rocks of the Wangshan Fm passed a fold test, the corresponding pole being at 26.1°N, 320.3°E ($A_{95} = 5.2°$). The sample-level mean direction of the ~925 Ma sill provides a virtual geomagnetic pole (VGP) position of 30.9°S, 136.2°E, dm/dp = 4.0°/2.4°, being antipodal to the pole of the Wangshan Fm. We interpreted that the two rock units have the same age and their mean pole likely represents the primary remanences. A paleomagnetic pole position of 54.0°S, 107.3°E ($A_{95} = 4.0°$) is obtained from the Jiayuan Fm, by averaging the site-level VGPs. This pole is of dual polarity and consistent with those published poles from this formation and other three carbonate formations in the middle part of Huaibei Group, but differs from any younger poles obtained in the region. We also interpreted it as of a primary remanence. Our new data, together with the published poles, depicted a loop-like segment of apparent polar wander path of the NCC, with an apex at ~925 Ma. It is termed as the "Huaibei loop" herein. The comparison between the "Huaibei loop" and the "Sveconorweigian loop", aided by the "right-way up" model of Laurentia–Baltica connection, indicates the paleogeographic proximities of the NCC to Laurentia, and probably to Siberia as well, in the supercontinent Rodinia.

1. Introduction

The question like how did the North China Craton (NCC) connect with other paleocontinents in the Precambrian supercontinents, e.g. Nuna (Columbia) and Rodinia, is of great interest to geologists in multiple research fields. Numerous models, often conflicting with each other, have been proposed and no consensus has been reached. Paleomagnetism remains the most powerful tool to test these models, but recent geochronological progress in the NCC (Su et al., 2012; Li et al., 2013 and references therein) suggested that most high quality Precambrian paleomagnetic poles of the NCC are older than ~1.30 Ga (Halls et al., 2000; Wu et al., 2005; Pei et al., 2006; Zhang et al., 2000, 2006, 2012; Chen et al., 2013; Xu et al., 2014). It means that the separation path of the NCC from Nuna and its paleogeographic position in Rodinia cannot be paleomagnetically constrained by available data.

* Corresponding author: State Key Laboratory of Biogeology and Environmental Geology, China University of Geosciences, Beijing 100083, China. Tel.: +86 10 82322257; fax: +86 10 82321983.
E-mail address: shzhang@cugb.edu.cn (S. Zhang).

http://dx.doi.org/10.1016/j.precamres.2015.08.013
0301-9268/

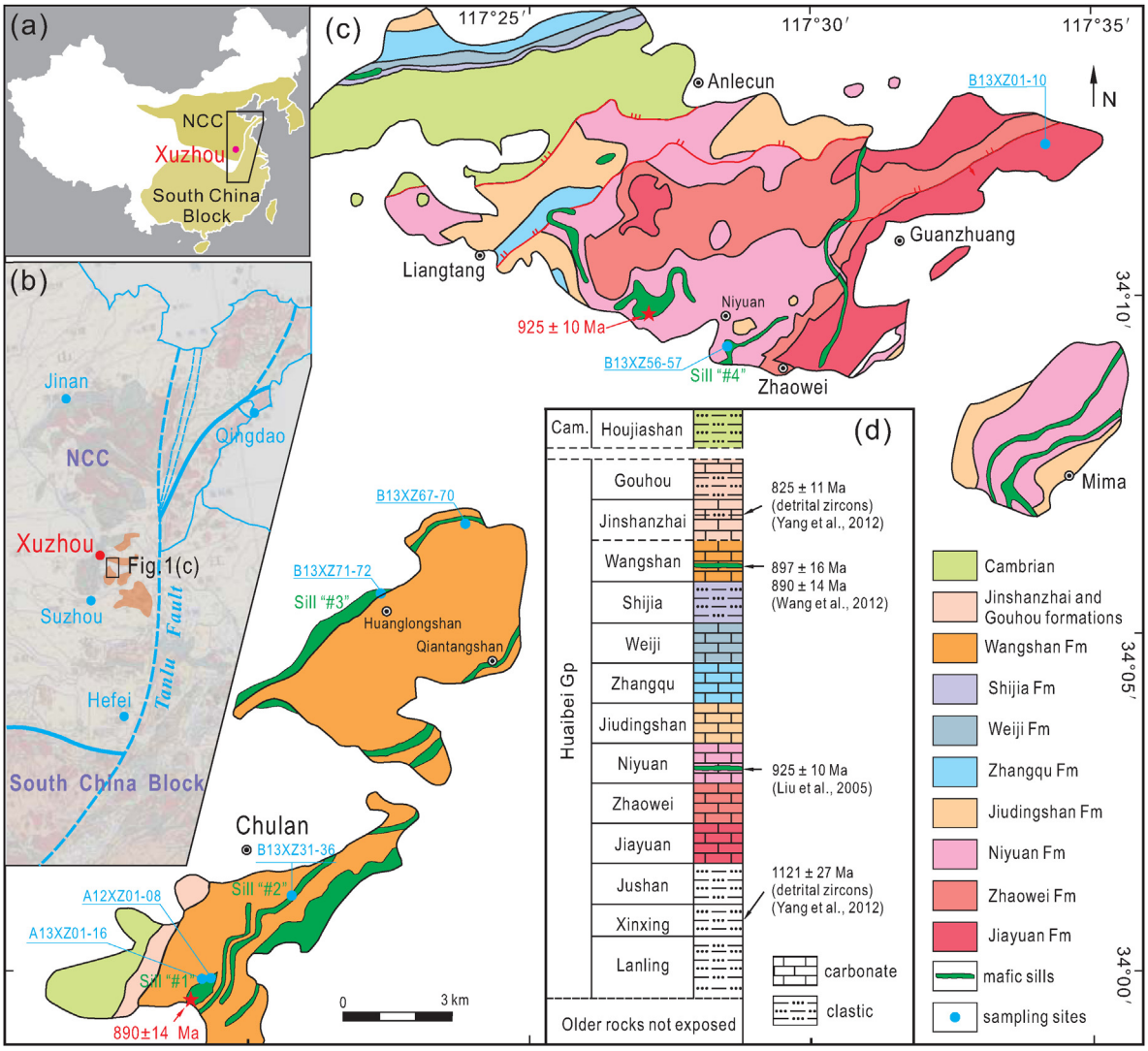

Fig. 1. (a) and (b) showing tectonic position of the NCC (North China Craton) and the study region. (c) Geological map of the Huaibei region showing the paleomagnetic sampling location. (d) The stratigraphy of the Huaibei Group, with geochronological constraints.

In this paper, we report new paleomagnetic results obtained from the Huaibei Group, exposed at the southeastern margin of the NCC (Fig. 1), and the Precambrian mafic sills that intruded into the Huaibei Group. Newly published U–Pb zircon dates, biostratigraphic and chemostratigraphic analyses indicate that the age of the lower to middle part of the Huaibei Group and the sills is between ~1120 and ~890 Ma (Liu et al., 2006; Wang et al., 2012; Yang et al., 2012; Xiao et al., 2014). Our new data provide important paleolatitudinal information for the NCC in this time interval, and allow us to reconstruct the paleogeographic position of the NCC in Rodinia.

2. Geological background

2.1. Strata

The Huaibei Group is a suite of siliciclastic and carbonate rocks (Cao et al., 1985; Xing, 1989; Xiao et al., 2014), exposed in the northern Jiangsu and Anhui Provinces (also known as the Xuhuai region), southeastern margin of the NCC (Fig. 1a and b). It is subdivided into 13 formations (Fig. 1c and 1d).

The lower part of the Huaibei Group is dominated by siliciclastic rocks (Fig. 1d). The Lanling Formation (Fm) is characterized by cross-stratified quartz sandstone; the Xinxing Fm consists of gray shale with carbonate concretions, and the Jushan Fm is composed of thick- to medium-bedded quartz sandstone (Cao et al., 1985).

The middle-upper Huaibei Group consists mainly of carbonate rocks. The ~450-m-thick Jiayuan Fm, overlying quartz sandstone of the Jushan Fm, consists of silty limestone, argillaceous limestone, and calcareous shale. The ~200-m-thick Zhaowei Fm overlies the Jiayuan Fm. It consists of thick-bedded, dark gray limestone with molar tooth structures in the lower part, and thin-bedded ribbon rocks (limestone with interbedded calcareous mudstone) in the upper part. The overlying Niyuan Fm, up to 600 m thick in places, consists of thick-bedded, yellowish gray dolomitic limestone in the lower part and dolostone in the upper part. The Jiudingshan Fm, overlying the Niyuan Fm, consists of thick-bedded, light gray stromatolitic and microbial dolostone. The succeeding Zhangqu Fm is ~300 m thick and consists of a 1-m-thick intraclastic limestone at the base, thin-bedded light gray micritic limestone in the lower part, and medium-bedded microcrystalline dolostone in the upper part. The ~300-m-thick Weiji Fm, overlying the Zhangqu Fm, consists of medium-bedded light gray dolostone in the lower part, and thick-bedded light gray and red dolomitic limestone with stromatolites in the upper part. The Shijia Fm is characterized by light gray and reddish purple shale with interbeds of stromatolitic dolostone (Cao et al., 1985; BGMRAP, 1987). The Wangshan Fm is ~500 m

Table 1
Paleomagnetic results of the ~890 Ma sills intruding into the Wangshan Formation near Xuzhou, Jiangsu Province.

Site	$N/N_0/(n)$	In geographic coordinates							In stratigraphic coordinates						
		D (°)	I (°)	K	α_{95} (°)	Plat (°N)	Plon (°E)	dm/dp A_{95} (°)	D (°)	I (°)	K	α_{95} (°)	Plat (°N)	Plon (°E)	dm/dp A_{95} (°)
Sill #1 (33°59′47″N, 117°19′19″E), near Chulan															
A12XZ02	6/6	329.2	11.9	46.8	9.9	50.1	349.8	10.1/5.1	328.0	−6.3	46.8	9.9	42.2	342.8	9.9/5.0
A12XZ03	7/9	342.1	18.8	23.7	12.7	60.6	335.5	13.2/6.9	340.4	2.2	23.7	12.7	52.3	330.6	12.7/6.4
A12XZ05	5/6	344.6	12.5	37.0	12.7	58.9	328.0	12.9/6.6	343.8	−3.7	37.0	12.7	51.0	323.6	12.7/6.4
A12XZ08	7/8	339.6	20.7	30.6	11.1	60.2	340.8	11.7/6.1	337.8	3.7	30.6	11.1	51.7	334.9	11.1/5.6
Average for sill #1 on site-level	(4)	338.2	15.8	114.0	8.6	57.7	339.2	A_{95} = 8.1	336.9	−1.4	104.3	9.0	49.5	333.4	A_{95} = 8.1
Average for sill#1 on specimen-level	25	338.8	16.5	28.8	5.5	57.8	339.5	5.7/2.9	337.6	−0.6	28.8	5.5	49.8	333.5	5.5/2.8
Sill #2 (34°01′02″N, 117°20′29″E), near Chulan															
B13XZ31	9/10	169.0	−18.2	275.1	3.1	−63.3	142.2	3.2/1.7	167.2	−7.8	275.1	3.1	−57.6	141.7	3.1/1.6
B13XZ32	6/6	168.0	−18.4	156.0	5.4	−63.1	144.2	5.6/2.9	166.3	−7.8	156.0	5.4	−57.3	143.3	5.4/2.7
B13XZ33	6/6	162.8	−17.9	387.8	3.4	−60.6	153.8	3.5/1.8	161.3	−6.8	387.8	3.4	−54.8	151.0	3.4/1.7
B13XZ34	12/12	163.9	−19.6	294.4	2.5	−61.9	152.7	2.6/1.4	162.1	−8.7	294.4	2.5	−56.0	150.6	2.5/1.3
B13XZ35	5/8	161.6	3.2	59.2	10.0	−50.4	147.0	10.0/5.0	162.7	14.2	59.2	10.0	−45.6	142.3	10.2/5.2
Average for sill #2 on site-level	(5)	165.0	−14.2	63.0	9.7	−59.9	148.0	A_{95} = 5.6	163.9	−3.4	63.0	9.7	−54.3	145.7	A_{95} = 5.3
Average for sill #2 on specimen-level	38	165.3	−15.9	69.5	2.8	−60.8	148.3	2.9/1.5	163.9	−5.1	69.5	2.8	−55.2	146.3	2.8/1.4
Sill #3 (34°05′30″N, 117°22′25″E), near Huanglongshan															
B13XZ71	11/11	161.3	19.2	61.1	5.9	−42.6	142.8	6.2/3.2	159.5	−3.7	61.1	5.9	−52.5	152.5	5.9/3.0
B13XZ72	11/11	165.6	21.2	165.1	3.6	−42.9	136.9	3.8/2.0	163.0	0.9	165.1	3.6	−51.9	145.7	3.6/1.8
Average for sill #3 on specimen-level	22	163.4	20.2	87.1	3.3	−42.8	139.9	3.5/1.8	161.3	−2.3	87.1	3.3	−52.7	149.3	3.3/1.7
Average for all sills on site-level[a]	(11)	**342.5**	**8.8**	**24.3**	**9.4**	**−56.3**	**150.0**	A_{95} = 5.5	**341.1**	**1.4**	**85.3**	**5.0**	**52.3**	**329.3**	A_{95} = 3.5
Average pole on sill-level: "N = 3"													52.6	330.0	A_{95} = 5.3

$N/N_0/(n)$, number of samples for statistic/number of samples for demagnetization/sites for statistics; D, declination; I, inclination; K, Fisher precision parameter of the mean; α_{95}/A_{95}, radius of circle of 95% confidence about the mean direction/pole; Plat/Plon, latitude/longitude of VGP; dm/dp, semi-axes of elliptical error around the pole at a probability of 95%.

[a] All 11 sites jointly pass a reversal test (McFadden and McElhinny, 1990), class C, with a critical angle 10.0°, angular difference is 7.0°, and a fold test by McFadden (1990), Definition 2.

thick (Cao et al., 1985; BGMRAP, 1987) and the strata consist of thin- to medium-bedded dolostone and limestone, with abundant stromatolites and molartooth structures (Cao et al., 1985; Meng and Ge, 2004; Liu et al., 2010; Jia et al., 2011). The Jinshanzhai Fm consists of glauconitic quartz sandstone, greenish gray shale, glauconitic limestone, and stromatolitic dolostone. The Jinshanzhai Fm is parallel disconformably overlying the Wangshan Fm. The Gouhou Fm is ~100 m thick and characterized by red and yellowish green shale and siltstone, with minor dolostone interbeds in the upper part.

The lower Cambrian Houjiashan Fm disconformably overlies the Gouhou Fm. The Houjiashan Fm has a thin phosphorite at the base, followed by thick-bedded limestone.

2.2. Mafic sills

In the study area, layer-parallel giant mafic sills, intruded into different formations of the Huaibei Group, with the latest horizon at the bottom of the upper Jinshanzhai Fm. In this study, paleomagnetic samples were collected from the mafic sills that intruded into the Wangshan and Niyuan formations (Fig. 1c). The sills are 10–200 m thick, generally more than 10 km in length and distributed in a NE–SW outcrop pattern (Fig. 1c). They are composed mainly of diabase. The carbonate host rocks near the sills have weak marbleization or skarnization. The sills sometimes display amygdaloidal structure at the top, columnar joints at the edges and the spheroidal weathering on the surface.

2.3. Age constraints of the sills and the Huaibei Group

At least two age groups of mafic sills intruding the Huaibei Group have been dated using zircon U–Pb analyses. The two groups have significantly different petrological and geochemical characteristics (Wang et al., 2012) and yield distinguishable paleomagentic remanence (see discussion in Section 4.3, this study). The younger sills intruding the Wangshan Fm at Langan (33°58.551′N, 117°18.320′E) were dated as 896.6 ± 16.3 Ma (Zircon, SHRIMP analyses, weighted mean $^{206}Pb/^{238}U$ age) and 890 ± 14 Ma (Zircon, LA-ICP-MS analyses, weighted mean $^{206}Pb/^{238}U$ age) (Fig. 1b) (Wang et al., 2012). The older mafic sills intruding the Niyuan and Jiudingshan formations, however, yield more complex age data (Liu et al., 2006; Gao et al., 2009). At a section 3 km west of the Niyuan village (Fig. 1b, 34°09.76′N, 117°27.01′E), sills occur within the Niyuan Fm and two samples from these sills were dated (Liu et al., 2006). Their zircon U–Pb ages were interpreted as 976 ± 24 Ma (T0398-1) and 1038 ± 26 Ma (T0398-2), respectively, both being weighted mean $^{207}Pb/^{206}Pb$ dates of SHRIMP analyses (Fig. 3 in Liu et al., 2006). However, the concordia plot of the sample T0398-2 shows very complex radiogenic lead loss. We thus consider that the weighted mean $^{207}Pb/^{206}Pb$ date (1038 ± 26 Ma) from this sample cannot represent the age of the sill. For the sample T0398-1, the U–Pb analyses are much more concordant. But considering the larger errors of the ^{207}Pb analyses (Table 1 in Liu et al., 2006), we recommend to use the weighted mean $^{206}Pb/^{238}U$ date as representative for the age of the sill. Our recalculation indicates that it should be 924.5 ± 9.5 Ma, if all the concordant analyses are included (n = 27, MSWD = 1.4). This does not conflict with the age reported by Liu et al. (2006) in their original analyses. This sill was dated again using SHRIMP zircon U–Pb method by Gao et al. (2009), giving a weighted mean $^{206}Pb/^{238}U$ date of 930 ± 10 Ma (n = 13, MSWD = 0.62). These analyses show that the older sills intruding into the Xuhuai Group are coeval with the ~925 Ma mafic dykes in other parts of the NCC reported by Peng et al. (2011).

No volcanic ash beds have been found to directly date the Huaibei Group, but some detrital zircon analyses have been published (Yang et al., 2012). The youngest detrital zircon population

Table 2
Paleomagnetic results of the Wangshan Formation near Xuzhou, Jiangsu Province.

Site	$N/N_0/(n)$	In geographic coordinates							In stratigraphic coordinates						
		D (°)	I (°)	K	α_{95} (°)	Plat (°N)	Plon (°E)	dm/dp A_{95} (°)	D (°)	I (°)	K	α_{95} (°)	Plat (°N)	Plon (°E)	dm/dp A_{95} (°)
Chulan section (33°59′45″N, 117°19′12″E)															
A13XZ03	5/5	324.1	−29.5	177.6	5.8	29.6	337.8	6.4/3.5	329.6	−53.8	177.6	5.8	16.0	323.1	8.1/5.7
A13XZ12	4/4	322.5	−29.4	55.6	12.4	28.8	339.3	13.7/7.6	325.7	−43.9	117.6	8.5	22.0	330.5	10.6/6.6
A13XZ13	4/4	335.6	−21.6	55.1	12.5	39.2	328.8	13.2/7.0	340.7	−38.6	55.1	12.5	31.3	318.4	14.9/8.8
A13XZ14	5/5	331.6	−25.9	492.8	3.5	35.2	331.8	3.8/2.0	335.5	−47.1	471.1	3.5	23.5	320.8	4.5/2.9
A13XZ15	7/7	337.4	−28.0	170.4	4.6	36.6	324.9	5.0/2.8	342.5	−39.9	170.4	4.6	30.9	316.2	5.5/3.3
A13XZ16	9/10	333.2	−25.4	41.2	8.1	36.2	330.2	8.7/4.7	332.5	−44.4	41.2	8.1	24.5	324.4	10.2/6.4
Average for Chulan section	(6)	330.8	−26.7	170.9	5.1	34.4	332.3	A_{95} = 5.1	334.7	−45.4	147.7	5.5	24.8	322.4	A_{95} = 6.1
Huanglongshan section (34°06′35″N, 117°23′50″E)															
B13XZ67	7/11	355.9	−62.7	105.4	5.9	11.7	300.4	9.2/7.2	350.0	−41.2	105.4	5.9	31.5	308.2	7.2/4.4
B13XZ68	3/10	348.1	−68.7	64.1	15.5	3.2	304.7	26.2/22.2	344.8	−46.8	64.1	15.5	26.1	312.3	20.0/12.9
B13XZ69-70	6/15	328.2	−61.9	28.5	12.8	7.4	320.2	19.8/15.4	331.8	−39.1	27.6	13.0	27.6	327.0	15.5/9.3
Average for Huanglongshan section	(3)	343.7	−64.9	121.8	11.2	6.1	320.9	A_{95} = 32.6	342.0	−42.6	100.7	12.4	28.6	315.9	A_{95} = 13.9
Average on site-level[a]	(9)	333.3	−39.4	15.9	13.3	26.0	323.5	A_{95} = 12.2	337.2	−44.1	116.2	4.8	26.1	320.3	A_{95} = 5.2

Abbreviations are the same as in Table 1.
[a] Chulan and Huanglongshan results jointly pass a fold test of McFadden (1990), Definition 2.

Table 3
Paleomagnetic results for contact test from the Chuanlan section.

Site	$N/N_0/(n)$	In geographic coordinates				In stratigraphic coordinates			
		D (°)	I (°)	K	α_{95} (°)	D (°)	I (°)	K	α_{95} (°)
Baked carbonate of the Wangshan Formation									
A13XZ01	12/12	332.5	8.8	9.0	15.3	332.6	−8.6	9.0	15.3
A13XZ07	6/7	347.4	32.6	30.3	12.4	340.3	19.4	30.3	12.4
A13XZ11-12	9/10	331.0	−2.1	11.3	16.0	332.0	−14.0	11.6	15.8
Wangshan Formation									
A13XZ03	5/5	324.1	−29.5	177.6	5.8	329.6	−53.8	177.6	5.8
Average for Chulan section[a]	(6)	330.8	−26.7	170.9	5.1	334.7	−45.4	147.7	5.5
~890 Ma sill									
Average for Chulan section[b]	(4)	338.2	15.8	114.0	8.6	336.9	−1.4	104.3	9.0

Abbreviations are the same as in Table 1.
[a] 6-Site-average direction of the Wangshan Formation from the Chulan section, see Table 2.
[b] 4-Site-average direction of the ~890 Ma sill from the Chulan section, see Table 1.

of the sandstone from the Xinxing Fm has an average age of 1121 ± 27 Ma (n = 9; LA-ICP-MS analyses), with the youngest zircon that was dated of 1069 ± 27 Ma (Yang et al., 2012). The youngest detrital zircon populations of the sandstone from the Jinshanzhai Fm have average age of 925 ± 10 Ma (n = 8) and 825 ± 11 Ma (n = 4), respectively (LA-ICP-MS analyses, Yang et al., 2012).

Recently, based on the available isotopic ages and biostratigraphic and chemostratigraphic analyses, Xiao et al. (2014) suggested that the Huaibei group and its equivalents nearby are of early-middle Tonian age, not as young as Cryogenian or as old as Mesoproterozoic. In addition to a favorable interpretation of Tonian age for the microfossils, they suggested that the positive $\delta^{13}C_{carb}$ plateau from the upper part of the Huaibei Group could be correlated with the early-middle Tonian carbonates in Australia and Laurentia (Xiao et al., 2014, and references therein).

Based on these analyses, we consider that the lower part (From the Xinxing Fm to Zhaowei Fm) of the Huaibei Group is younger than ~1120 Ma (constrained by the average age of the youngest detrital zircon population) and is older than the ~925 Ma sills that intruded the strata. The Wangshan Fm is older than ~890 Ma and younger than ~1120 Ma. The Jinshanzhai Fm should be younger than ~825 Ma (constrained by the average age of the youngest detrital zircon population) and older than the Cambrian strata overlying it.

2.4. Structures

The study area is located in the western side of the Tanlu fault (Fig. 1b), which is considered to be a Mesozoic transform boundary between the NCC and the South China Block (Wang et al., 2005). The Cambrian strata and the undivided Archean–Paleoproterozoic basement rocks indicate that the study area is a coherent part of the NCC. The Huaibei Group, Precambrian sills and the Cambrian strata were all folded during the middle Jurassic (BGMRJP, 1984), but the disconformable parallel contact between the Cambrian and Huaibei Group indicate that the Precambrian strata had not been tilted until after Cambrian time.

3. Paleomagnetic sampling

The first paleomagnetic investigation of the Huaibei Group was carried out over thirty years ago by Fang et al. (1983). Instruments and technique used in that time were rather simple but their report is still valuable. Zhang et al. (2000, 2006) have reviewed those data and suggested that: (1) the paleopoles derived from the Jinshanzhai, Wangshan, Shijia, Weiji, Jiudingshan formations are close to each other and similar to the late Mesozoic to Cenozoic poles of the NCC, so they likely represent Mesozoic to Cenozoic overprints; (2) the data obtained from the Zhangqu, Niyuan, Zhaowei, Jiayuan formations are acceptable in spite of the small number of samples.

Samples were collected from three ~890 Ma sills (sill "#1", "#2" and "#3" in Fig. 1c) and one ~925 Ma sill (sill "#4" in Fig. 1c) and the Wangshan and Jiayuan formations, using a gasoline-powered drill and were oriented using a magnetic compass and a sun compass when possible. No significant difference was observed between the results using the two orientation devices. Samples that were measured and used in statistics are listed on site-level in individual tables (Tables 2–5) for each rock-unit, with their GPS information that corresponds to the sampling locations in Fig. 1c.

4. Paleomagnetic experiments, analyses and results

4.1. Laboratory conditions and procedures

All experiments were conducted in the Paleomagnetism and Environmental Magnetism Laboratory of China University of Geosciences, Beijing (CUGB). Diabase core samples were cut into ~0.7 cm thick specimens, and carbonate core samples were cut into ~2.2 cm thick specimens. Specimens and instruments were kept in a μ-metal shielded room during the demagnetization process, with ambient magnetic fields typically 100–300 nT in the sample loading, transfer, and storage regions, and <10 nT in the magnetometer measurement and furnace heating/cooling zones.

After measurements of the natural remanent magnetization (NRM), alternating field demagnetization was performed on only a few specimens. Since only soft components could be isolated and no stable hard component was gained during AF demagnetizations, almost all specimens were subjected to step-wise thermal demagnetizations. These demagnetizations were conducted at temperatures of 80, 120, 150, 200, 300, 350, 400, 450, 480, 510, 530, 540, 550, 560, 565, 570, 575, 580, 585, 590, 600, 620 °C, until the remanence directions became unstable. The thermal demagnetization was carried out using a TD-48 thermal demagnetizer. Remanent magnetizations of 24 diabase samples from the sill "#1" were measured using a JR-6A spinner magnetometer. Remanent magnetizations of the other samples were measured using a 2G 755-4K superconducting magnetometer.

4.2. Paleomagnetic results

4.2.1. Paleomagnetism of the ~890 Ma sills

The NRM intensities of the specimens of the ~890 Ma sills range between 0.1 and 1 A/m. Two components were identified using principal component analysis (PCA) (Kirschvink, 1980).

A low unblocking temperature component (LTC) was identified and erased in temperature below 350 °C in most cases (Fig. 2a–d) The LTC directions (*in situ*) of the specimens from the sill "#1"

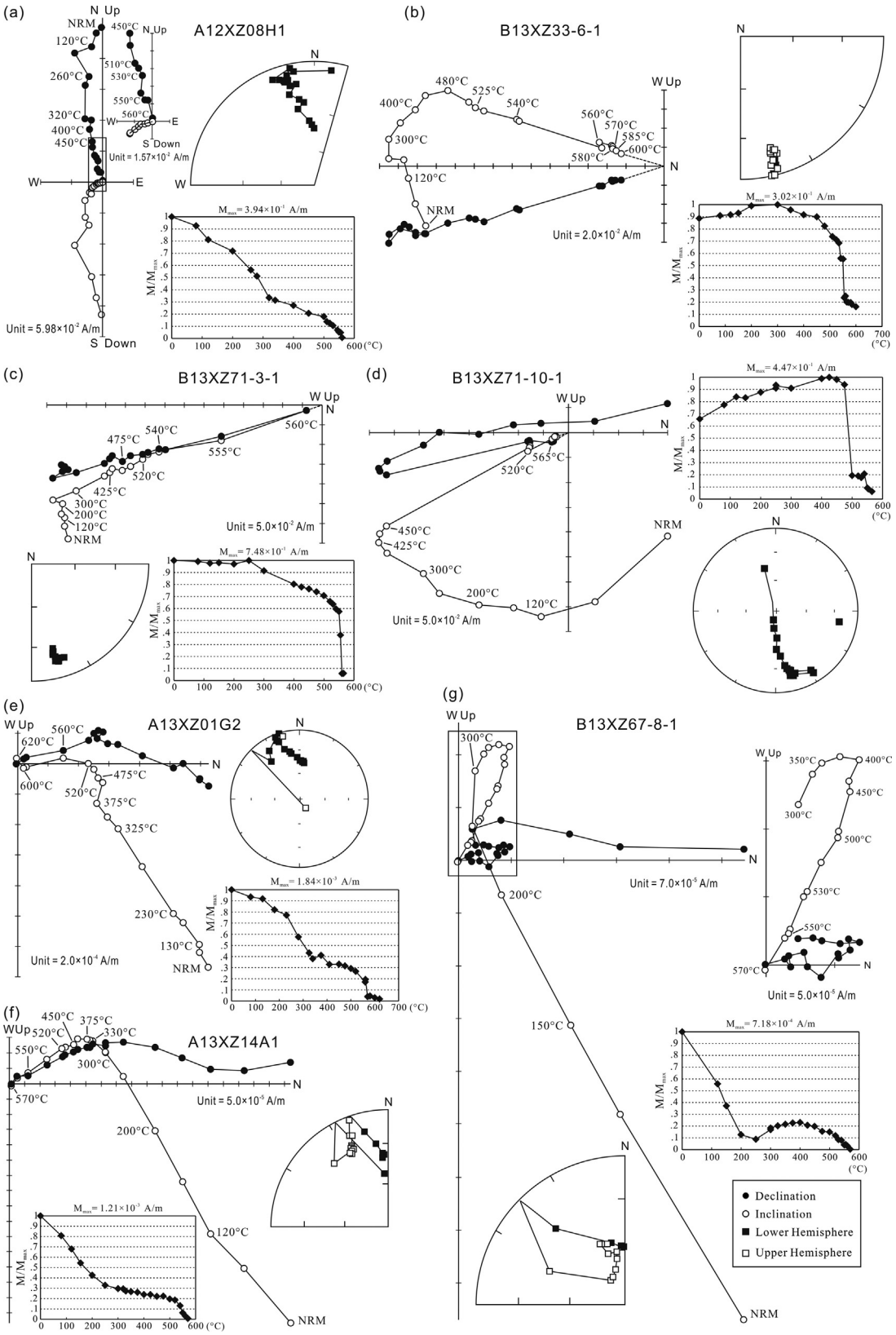

Fig. 2. Examples of magnetic behavior during thermal demagnetizations of diabase specimens from the ca 890 Ma sills of the sill "#1" (a), the sill "#2" (b), and the sill "#3" (c and d), respectively. The magnetic behavior during thermal demagnetization of a carbonate specimen of the Wangshan baked by the sill "#1" (e) and of carbonate specimen from the Wangshan Fm collected in the Chulan (f) and the Huanglongshan (g) sections. The directions of remanence are all in geographic coordinates.

Table 4
Paleomagnetic results of the Jiayuan Formation near Xuzhou, Jiangsu Province (34°11′55.7″N, 117°34′1.3″E).

Site	$N/N_0/(n)$	In geographic coordinates							In stratigraphic coordinates						
		D (°)	I (°)	K	α_{95} (°)	Plat (°N)	Plon (°E)	dm/dp A_{95} (°)	D (°)	I (°)	K	α_{95} (°)	Plat (°N)	Plon (°E)	dm/dp A_{95} (°)
B13XZ01	10/10	187.1	42.0	26.5	9.6	−31.2	109.9	11.8/7.2	178.6	16.9	26.5	9.6	−47.1	119.5	9.9/5.1
B13XZ02	8/8	191.2	39.7	40.7	8.8	−32.3	105.4	10.6/6.3	186.6	9.3	40.7	8.8	−50.6	107.2	8.9/4.5
B 13XZ04	5/5	189.3	38.5	97.3	7.8	−33.4	107.1	9.3/5.5	185.1	10.8	97.3	7.8	−50.1	109.6	7.9/4.0
B 13XZ05	5/5	187.0	3.2	30.8	14.0	−53.6	105.7	14.0/7.0	188.4	−18.9	30.8	14.0	−64.3	98.1	14.6/7.6
B 13XZ06	7/7	188.9	27.1	60.8	7.8	−40.7	106.1	8.5/4.6	186.1	5.0	60.8	7.8	−57.8	106.0	7.8/3.9
B 13XZ07	4/5	188.3	32.0	172.0	7.0	−37.8	107.5	7.9/4.4	184.1	2.7	172.0	7.0	−54.2	110.5	7.0/3.5
B13XZ08	5/5	191.2	30.5	57.6	10.2	−38.3	103.8	11.4/6.3	186.9	1.9	57.6	10.2	−54.3	105.6	10.2/5.1
B13XZ09	7/7	194.5	27.6	206.8	4.2	−39.2	99.3	4.6/2.5	190.3	6.4	206.8	4.2	−51.4	100.9	4.2/2.1
B13XZ10	9/10	191.8	20.6	30.5	9.5	−43.8	101.3	10.0/5.2	187.5	−0.3	29.6	9.6	−55.2	104.3	9.6/4.8
Average on site-level	(9)	189.9	29.1	45.6	7.7	−39.4	105.2	8.5/4.7	186.0	3.8	60.2	6.7	−53.5	107.5	6.7/3.4
Average pole for the Jiayuan Formation on site-level						−38.9	105.2	A_{95} = 4.7					−54.0	107.3	A_{95} = 4.0

Abbreviations are the same as in Table 1.

Table 5
Paleomagnetic results of the ~925 Ma sill near Xuzhou, Jiangsu Province (34°08′57.0″N, 117°28′26.0″E).

Site	N/N_0	In geographic coordinates							In stratigraphic coordinates						
		D (°)	I (°)	K	α_{95} (°)	Plat (°N)	Plon (°E)	dm/dp (°)	D (°)	I (°)	K	α_{95} (°)	Plat (°N)	Plon (°E)	dm/dp (°)
B13XZ56	8/9	154.0	24.0	78.9	6.3	−37.1	150.0	6.7/3.6	165.4	40.2	78.9	6.3	−31.2	133.3	7.6/4.6
B13XZ57	10/10	150.6	21.9	155.2	3.9	−36.6	154.3	4.1/2.2	160.6	39.3	155.2	3.9	−30.6	138.4	4.7/2.8
Average on sample-level	18	152.1	22.8	108.0	3.3	−36.8	152.4	3.5/1.9	162.7	39.7	108.0	3.3	−30.9	136.2	4.0/2.4

Abbreviations are the same as in Table 1.

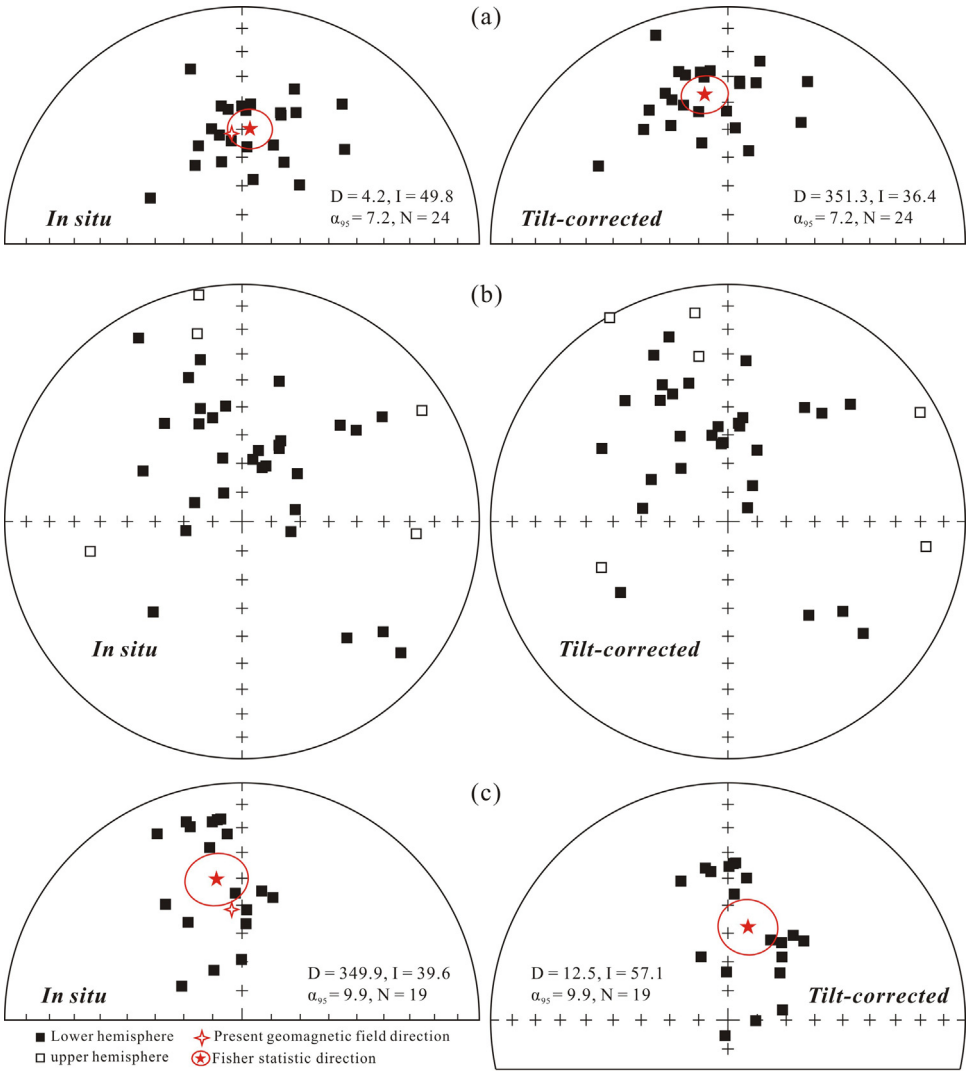

Fig. 3. Equal area projections of the low unblocking temperature component (LTC) directions isolated in the sill "#1" (a), the sill "#2" (b) and the sill "#3" (c).

and the sill "#3" concentrated around the present field direction (PFD) of this region (D = 354.5°, I = 51.3°, IGRF, online data) (Fig. 3a and c) and were thus interpreted as a viscous remanent magnetization (VRM) of the recent geomagnetic field. However, the LTC remanence directions of the specimens from the sill "#2"were distributed randomly (Fig. 3b).

Magnetic behaviors of the high unblocking temperature component (HTC) varied with the mineral size of the sills. Stable HTC directions were usually identified in the fine-grained sills, but could be occasionally identified in the coarse-grained sills. The unblocking temperature of the HTC is often near to the Curie temperature of magnetite (~575 °C, Fig. 2a–d), suggesting that it is probably carried by magnetite.

The sill "#1" is coarse-grained diabase. We collected 54 samples from eight sites (A12XZ01-08, Fig. 1c), but the HTCs could only be isolated in 25 samples from 4 sites (Table 1). For the sill "#2", samples from site B13XZ36 were coarse diabase and the HTC directions were scattered. The HTC directions isolated in the samples from the other five sites of the sill "#2" (B13XZ31-35) and the two sites of the sill "#3" (B13XZ71-72) were stable and were all used for mean calculations.

These HTCs were of dual polarity (Fig. 4a). The northwestward directions were defined as polarity 1 and the southeastward directions as polarity 2. This component passed a reversal test of "C" Class (McFadden and McElhinny, 1990) and a fold test of McFadden (1990), Definition 2 (Table 1). The concentration of the remanence directions varied systematically as the strata were step-wise unfolded (Watson and Enkin, 1993). The precision parameter, k, of the mean remanence direction reached the highest value when the strata were unfolded to 98.5%, with the k_{max} = 85.4 and k = 24.3 in the geographic coordinate (Fig. 4b). This suggests that remanence recorded by the ~890 Ma diabase sills had been acquired before the beds were tilted.

The HTC site-mean direction of the sill "#1" is D_g = 338.2°, I_g = 15.8°, α_{95} = 8.6° in geographic coordinates and D_s = 336.9°, I_s = −1.4°, α_{95} = 9.0° in stratigraphic coordinates. The mean pole position in stratigraphic coordinates falls at 49.5°N, 333.4°E (A_{95} = 8.1°), by averaging the virtual geomagnetic poles (VGP) of all sites (Table 1). The HTC site-mean direction of the sill "#2" is D_g = 165.0°, I_g = −14.2°, α_{95} = 9.7° in geographic coordinates and D_s = 163.9°, I_s = −3.4°, α_{95} = 9.7° after tilt correction. The mean pole averaged from the VGPs of all sites in stratigraphic coordinates is located at 54.3°S, 145.7°E (A_{95} = 5.3°, Table 1). No site-mean HTC direction has been calculated for the sill "#3", since there are only two sites from this sill.

We use two methods to calculate the mean pole of the ~890 Ma sills: (1) by averaging all the VGP of each site from all sills, the mean paleomagnetic pole is at 52.3°N, 329.3°E (A_{95} = 3.5°, Table 1); (2) because only three separate sills were sampled, we calculate the mean as N = 3 intrusions. The pole is at 52.6°N, 330.0°E (A_{95} = 5.3°, Table 1). They are identical within error, but the method 2 presents slightly larger error, being better to represent the paleomagnetic record of the ~890 Ma sills.

4.2.2. Paleomagnetism of the Wangshan Fm

The samples of the Wangshan Fm are all carbonate rocks, including samples baked by the ~890 Ma sills and fresh dolomite samples (unbaked). In this subsection, we only discuss the results from the unbaked samples.

The NRM intensities of the samples from the Wangshan Fm are 0.5–10 mA/m. Two remanence components were identified. The LTC remanence was isolated and in most cases erased in temperatures below 300 °C (Fig. 2f and g). The directions of this component (*in situ*) are close to the PFD of the region (Fig. 5a and b) and this component is thus interpreted as a VRM of the recent geomagnetic field.

The HTC was identified in roughly 50% of the sampled sites, which include six sites in the Chulan section and four sites in the Huanglongshan section. In some cases, usually for the relatively pure dolomite layers, the magnetization intensities of most samples in a site were so low that it was not possible to identify any HTC, we did not include such a site in the paleomagnetic statistics. In the Huanglongshan section, sites B13XZ69 and B13XZ70 are very close to each other, and each has a few samples yielding the HTC, therefore, we combined them as one site in the statistics (Table 2).

In general, the isolated HTC has an unblocking temperature up to 570 °C (Fig. 2f and g), suggesting that magnetite is likely the magnetic carrier. The HTC was directed northwestward and moderately up after tilt correction (Fig. 6a). It is clearly different to the HTC of the ~890 Ma sills that intruded into the Wangshan Fm. The HTC of the Wangshan Fm also passed a fold test of McFadden (1990), Definition 2 (Table 2). The step-wise unfolding test indicated that the precision parameter, k, reached the highest value when the strata were unfolded to 93.3%, with the k_{max} = 120.1 and k = 15.9 in the geographic coordinate (Fig. 6b; Table 2). This suggests that the HTC recorded by the carbonate rocks of the Wangshan Fm was acquired before the folding.

The site-level (n = 6) average HTC direction of the Chulan section is D_g = 330.8°, I_g = −26.7°, α_{95} = 5.1° in geographic coordinates and D_s = 334.7°, I_s = −45.4°, α_{95} = 5.5° in stratigraphic coordinates. The mean paleomagnetic pole position in stratigraphic coordinates falls at 24.8°N, 322.4°E (A_{95} = 6.1°), by averaging the VGP of each site (Table 2). The HTC site-mean (n = 3) direction of the Huanglongshan section is D_g = 343.7°, I_g = −64.9°, α_{95} = 11.2° in geographic coordinates and D_s = 342.0°, I_s = −42.6°, α_{95} = 12.4° in stratigraphic coordinates. The mean paleomagnetic pole position calculated from the site mean VGPs is located at 28.6°N, 315.9°E (A_{95} = 13.9°, Table 2). The mean paleomagnetic pole position for the Wangshan Fm is at 26.1°N, 320.3°E (A_{95} = 5.2°, Table 2), by averaging the VGP of each site from the Chulan and Huanglongshan sections.

4.2.3. Contact test between the ~890 sills and Wangshan Fm

A contact test was successfully carried out in the Chulan section (Figs. 7 and 8). Sites A13XZ01, 07, 11 and 12 are situated up to ~3 m above the contact with the ~890 Ma sill (Fig. 8b). The carbonate rocks that were baked by the sills are whitish. The site A13XZ03 is situated far from the boundary (Fig. 8b) and seems lithologically distinct from the baked zone. The NRM intensities of the baked carbonate specimens of the Wangshan Fm are 0.1–1 mA/m. Two components were identified using PCA (Kirschvink, 1980). A LTC remanence was identified in temperatures below 400 °C in most cases (Fig. 2e) and the remanence directions (*in situ*) are close to the PFD of this region (Fig. 7a and b), so it is interpreted as a VRM of the recent geomagnetic field. A HTC magnetization could genetally be defined in temperatures between 560 and 620 °C in most cases. During the thermal demagnetization treatment, the remanence intensity decreased sharply at ~520 °C and then decreased in temperatures until 620 °C (Fig. 2e), indicating that magnetite and hematite may both exist in the samples.

The HTC directions of the baked carbonate rocks (sites A13XZ01, 07 and 11-12) are close to the site-level mean direction of the ~890 Ma sill (Fig. 8a, Table 3), but different from the site-level mean direction of the Wangshan Fm (Fig. 8a, Table 3). This suggests that the baked carbonate rocks were remagnetized during the process of the intrusion. On the contrary, the remanence directions after tilt correction of the unbaked samples (sites A13XZ03) are consistent with the remanence directions of the Wangshan Fm (Table 2), but different from the remanence directions of the ~890 Ma sills (Fig. 8a and c, Table 3). This indicates that the unbaked carbonate rocks of the Wangshan Fm were not remagnetized during the sill intrusion. This positive baked contact test strongly suggests that

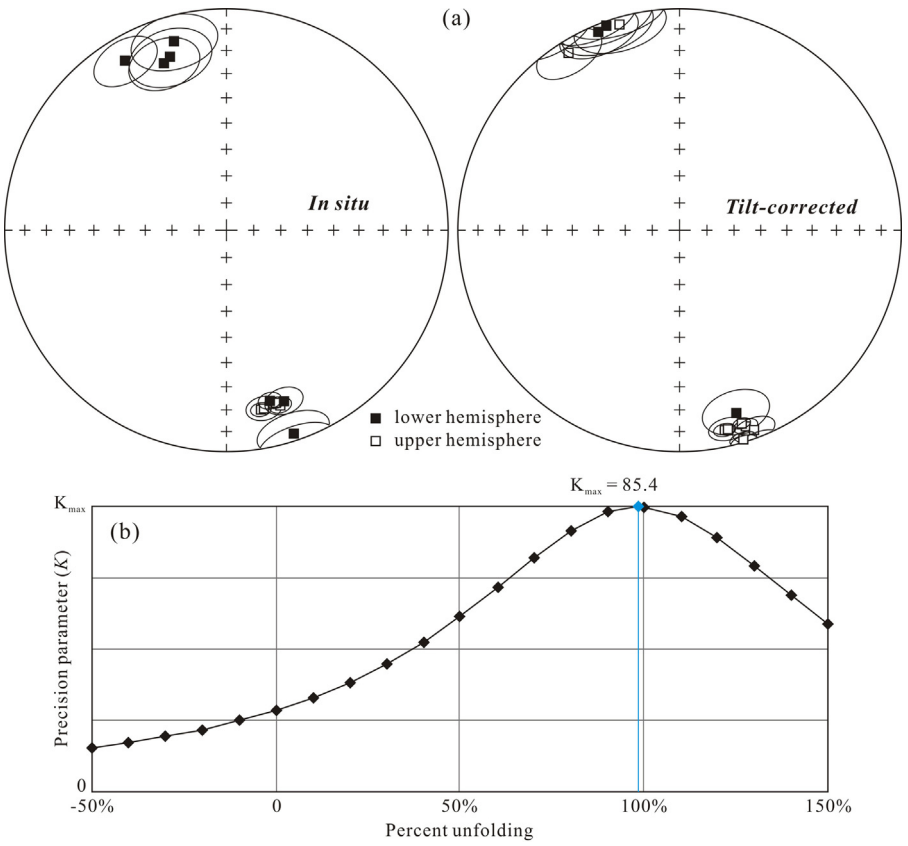

Fig. 4. (a) Equal area projections of the high unblocking temperature component (HTC) directions of the ~890 Ma sills before and after tilt correction. (b) Results of step-wise unfolding test (Watson and Enkin, 1993). The precision parameter (k) reaches the highest value when the strata are 98.5% unfolded, with k_{max} = 85.4 and k = 24.3 in geographic coordinate.

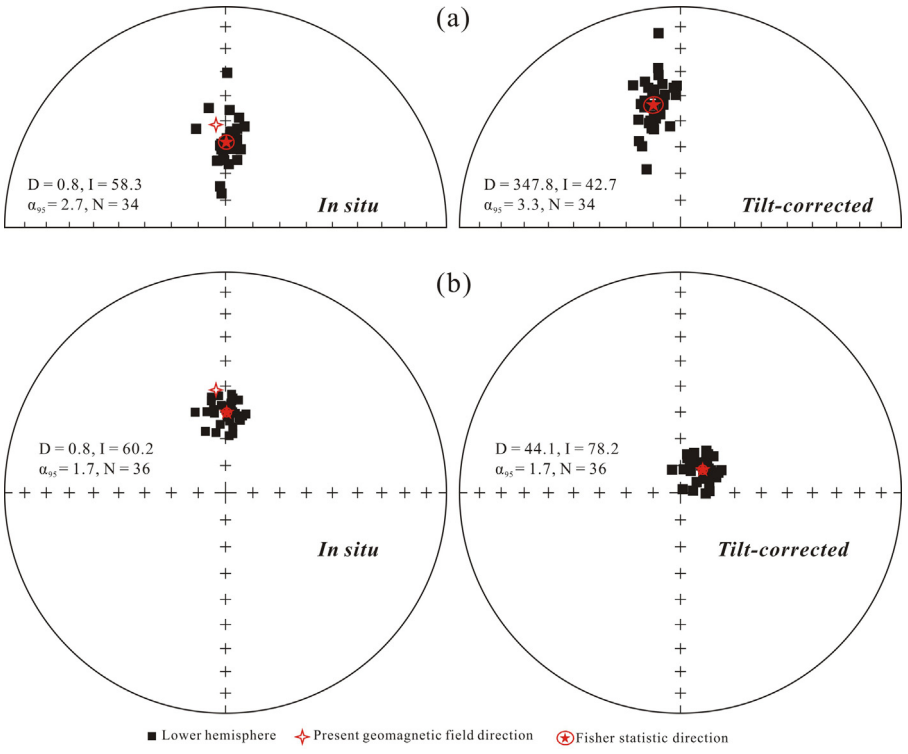

Fig. 5. The direction of the LTC remanence of the Wangshan Fm (shown in equal area projection) from the Chulan (a) and the Huanglongshan (b) sections.

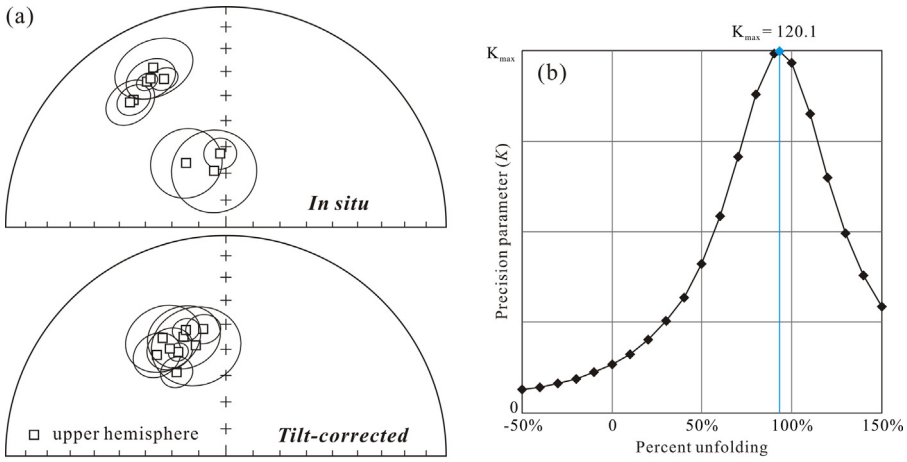

Fig. 6. (a) Equal area projections of the HTC directions of the Wangshan Fm before and after tilt correction. (b) Results of step-wise unfolding test (Watson and Enkin, 1993). The precision parameter (k) reach the highest value when the strata are 93.3% unfolded, with k_{max} = 120.1 and k = 15.9 in geographic coordinate.

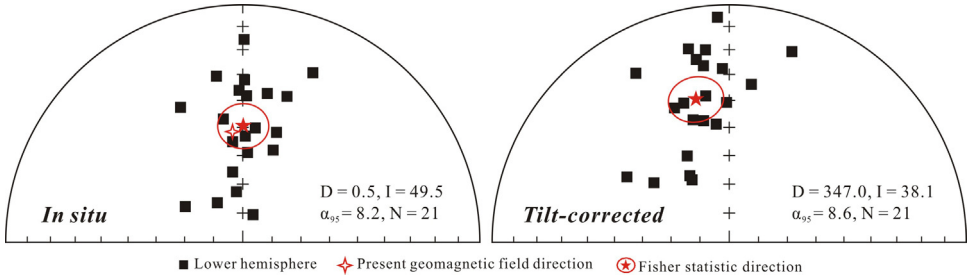

Fig. 7. The directions of the LTC remanence carried by baked carbonate rocks of the Wangshan Fm from the Chulan section.

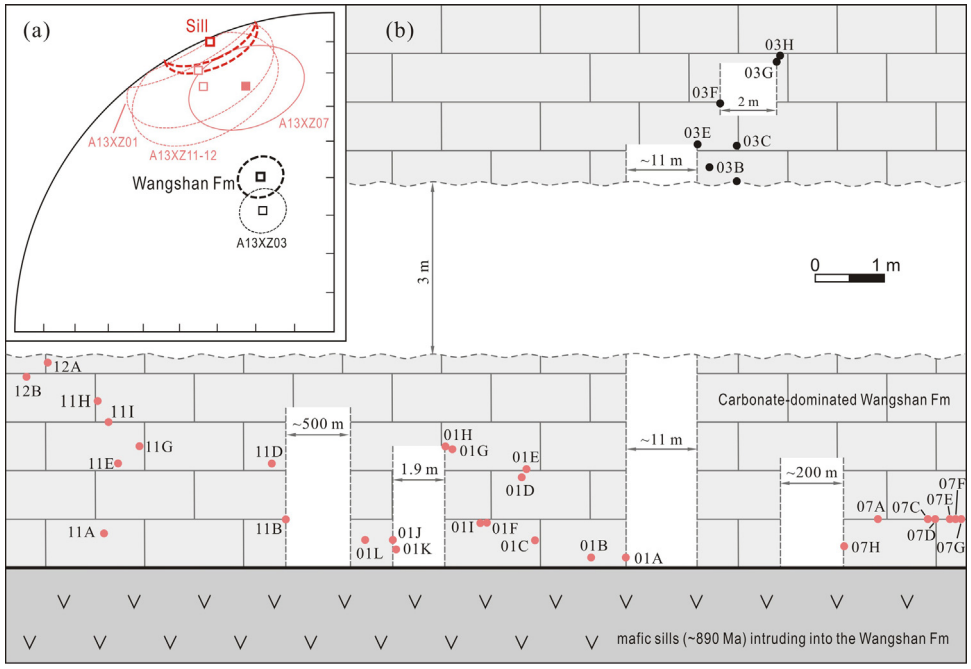

Fig. 8. (a) Baked contact test between the host rocks of the Wangshan Fm and the ~890 Ma sills, in the Chulan section. Equal area projections of the HTC directions of three sites of the baked carbonate rocks of the Wangshan Fm (A13XZ01, A13XZ07 and A13XZ11-12) are close to the mean direction of the diabase sill in this section; while they are obviously different from the mean direction of the Wangshan Fm in this region and the mean direction of the unbaked site A13XZ03, suggesting that the HTC of the baked carbonate rocks was a thermal overprint acquired during the intrusion of the ~890 Ma sills. (b) The distribution of samples of the three sites (A13XZ01, A13XZ07 and A13XZ11-12) of the baked carbonate rocks and the one site (A13XZ03) of the unbaked carbonate rocks of the Wangshan Fm.

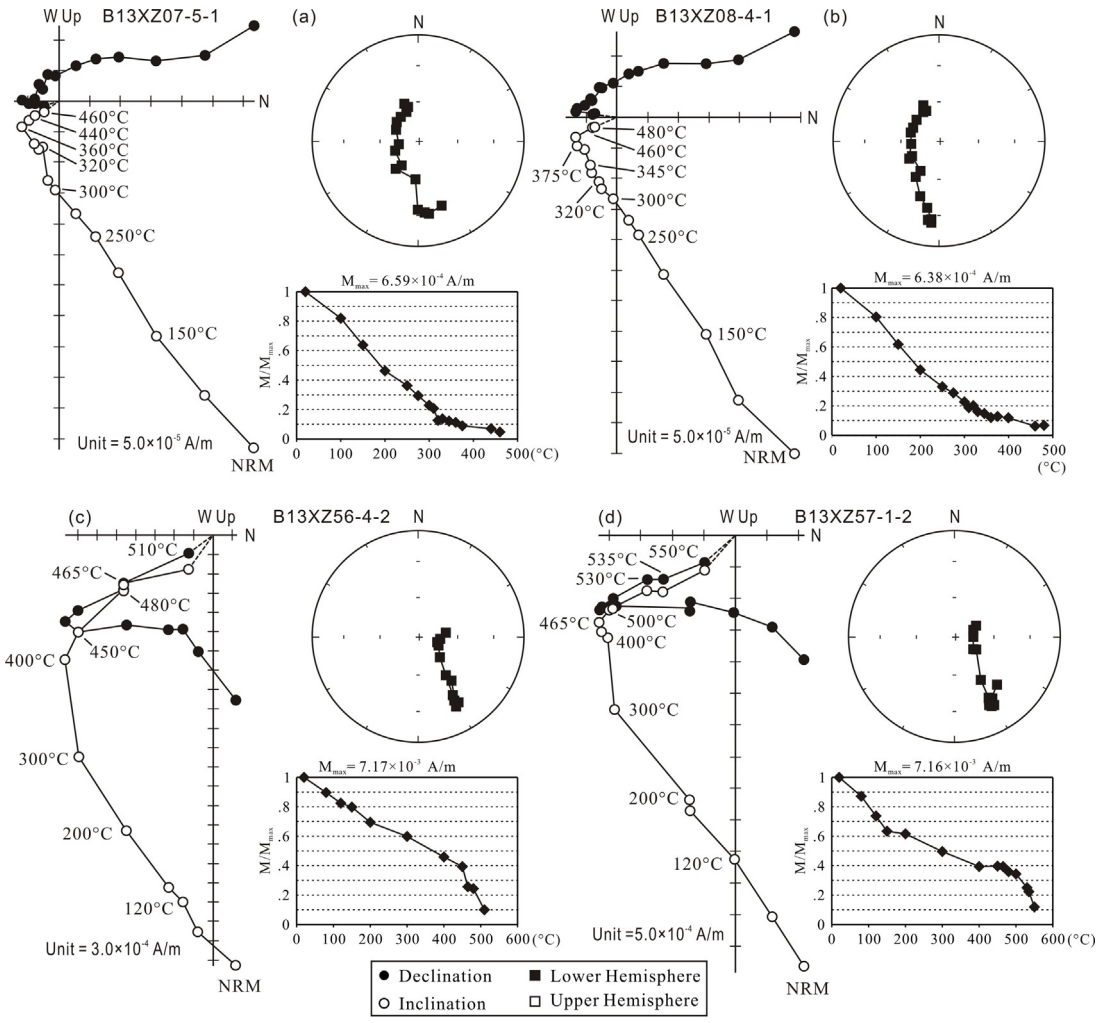

Fig. 9. Examples of remanence behavior during thermal demagnetization of specimens from carbonate rocks of the Jiayuan Fm (a, b) and from diabase specimens of the 925 Ma sills (c, d). The directions are in geographic coordinates.

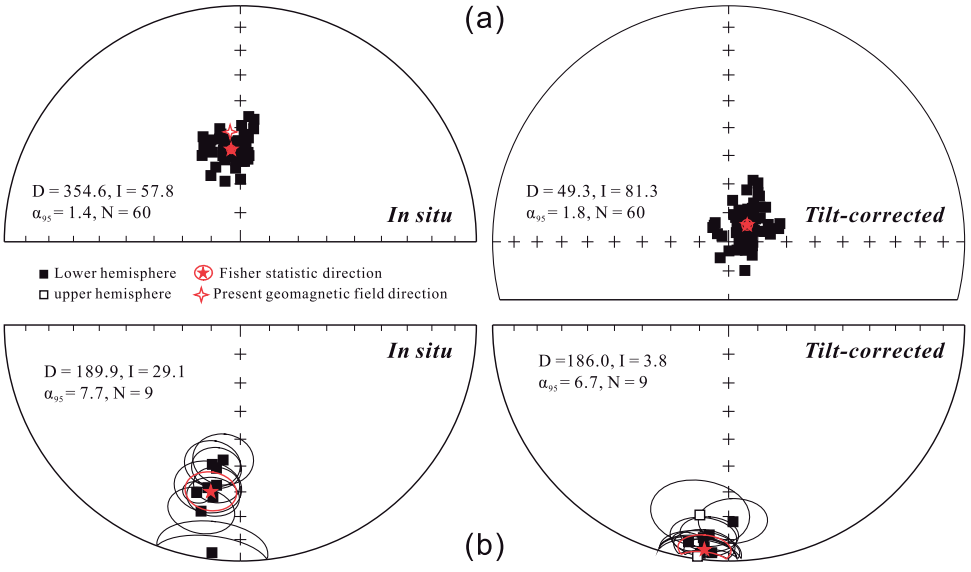

Fig. 10. The directions of the LTC (a) and the HTC (b) of the Jiayuan Fm. The directions are shown in an equal area projection.

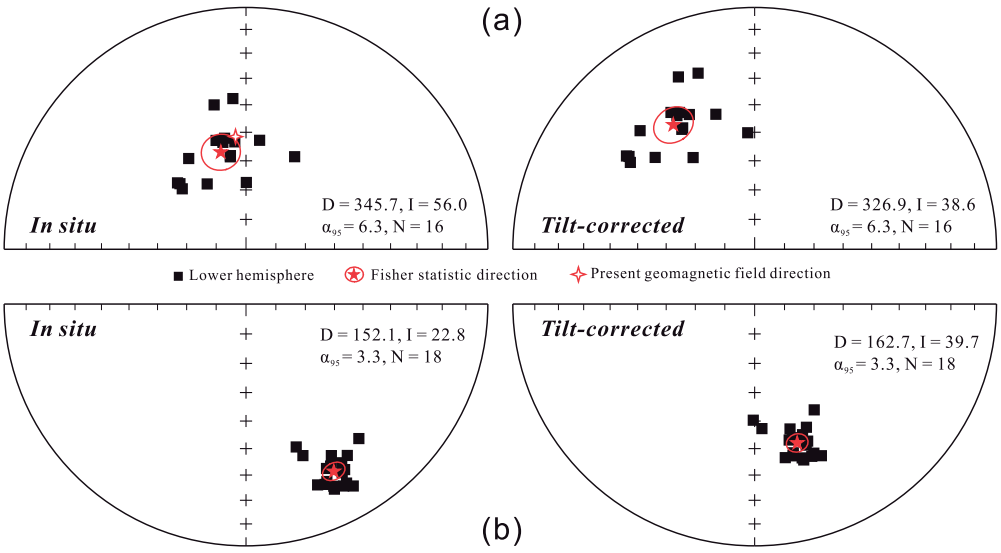

Fig. 11. The directions of the LTC (a) and the HTC (b) of the ~925 Ma sill. The directions are shown in an equal area projection.

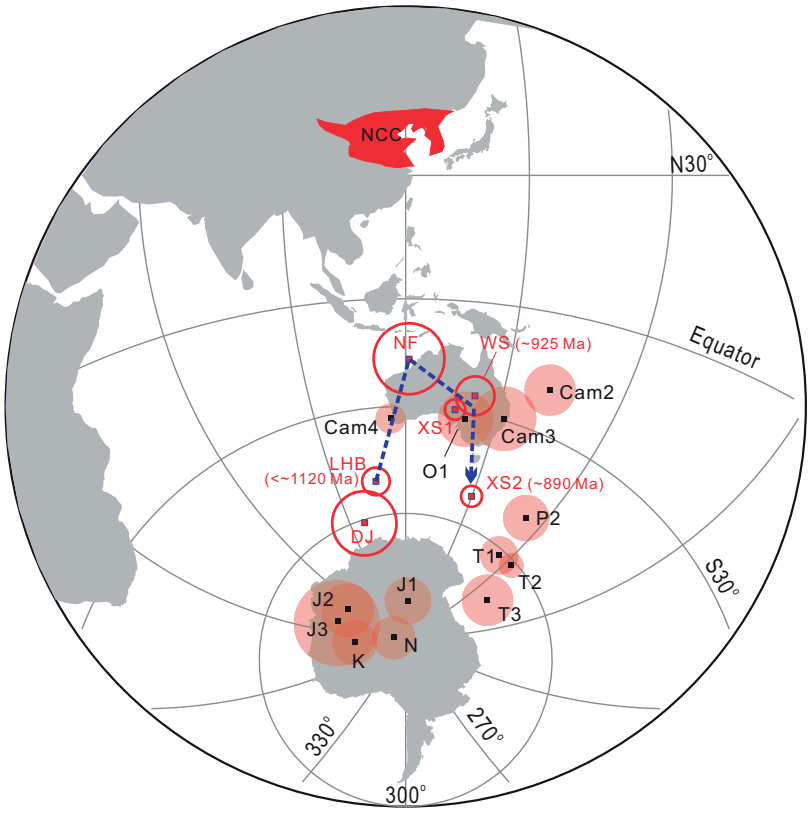

Fig. 12. Paleomagnetic poles and their confidence circles (A_{95}) with ages of ca. 1120–890 Ma (in red) showing the "Huaibei loop" and the younger poles of NCC are shown by the block sequences with pale-red A_{95}. More information of the "Huaibei loop" poles are listed in Table 6 and the Phanerozoic data selection is after Huang et al. (2008), but J3 data are from Ren et al. (2015). Geologic time abbreviations: Cam2/Cam3/Cam4, Series 2/3/4 of Cambrian; O1, Early Ordovician; P2, Late Permian; T1, Early Triassic; T2, Middle Triassic; T3, Late Triassic; J1, Early Jurassic; J2, Middle Jurassic; J3, Late Jurassic; K, Cretaceous; N, Cenozoic. The stratigraphic correlation of the Cambrian is after Zhu (2010). (For interpretation of the references to color in this figure legend, the reader is referred to the web version of this article.)

the HTC magnetization carried by the ~890 Ma sills is a primary remanent magnetization.

4.2.4. Paleomagnetism of the Jiayuan Fm

The NRM intensities of the carbonate rocks of the Jiayuan Fm are 0.1–1 mA/m. Two components of the remanent magnetizations were identified. The LTC was isolated in temperatures below 300 °C and a HTC defined in temperatures up to 480 °C (Fig. 9a and b). The LTC remanence directions (*in situ*) are close to that of the PFD of this region (Fig. 10a), which suggests that the magnetization is a VRM. The HTC is most probably carried by magnetite–tianomagnetite.

The site-level ($n = 9$) mean HTC direction of the Jiayuan Fm is $D_g = 189.9°$, $I_g = 29.1°$, $\alpha_{95} = 7.7°$ in geographic coordinates and $D_s = 186.0°$, $I_s = 3.8°$, $\alpha_{95} = 6.7°$ in stratigraphic coordinates (Fig. 10b), corresponding to a pole at 53.5°S, 107.5°E (dm/dp = 6.7°/3.4°, Table 4). A mean paleomagnetic pole can also be obtained by averaging the VGP of each site (Table 4), resulting in a pole position at 54.0°S, 107.3°E ($A_{95} = 4.0°$,

Table 4). The precision increasing slightly between geographic and stratigraphic coordinates, even though not significantly at 95% confidence level, should be a signal of positive fold test, though not conclusive.

4.2.5. Paleomagnetism of the ~925 Ma sill

The NRM intensities of these specimens are 1–10 mA/m. Two components of remanence were identified. One of which was removed in temperatures below 400 °C (Fig. 9c and d). This LTC remanence has directions close to that of the PFD of this region (Fig. 11a) and it is thus interpreted as VRM. A HTC remanent magnetization is identified with unblocking temperature up to 550 °C (Fig. 9c and d), indicating that magnetite is likely the major magnetic carrier.

Like that of the ~890 Ma sills, the remanence directions of the coarse-grained diabase are chaotic when the samples are heated in high temperatures and no HTCs could be obtained. Therefore, only the stable HTCs from the fine-grained diabase samples were used in the paleomagnetic statistics (Table 5).

The sample-level ($N = 18$) average HTC direction of the ~925 Ma sill is $D_g = 152.1°$, $I_g = 22.8°$, $\alpha_{95} = 3.3°$ in geographic coordinates and $D_s = 162.7°$, $I_s = 39.7°$, $\alpha_{95} = 3.3°$ in stratigraphic coordinates (Fig. 11b), corresponding to a VGP of 30.9°S, 136.2°E (dm/dp = 4.0°/2.4°, Table 5).

4.3. Origin and age of the remanence

In this study, we isolated four high unblocking temperature components (HTCs) from the Huaibei Group sedimentary rocks and the Neoproterozoic sills. The HTC magnetizations in the ~890 Ma sills passed a fold test, a reversal test and a baked contact test and the calculated pole is significantly different from any younger poles of the NCC (Fig. 12). We interpret this remanence component as primary.

The HTC of the carbonate rocks of the Wangshan Fm passed a fold test. Although the fold was formed during middle Jurassic time (BGMRJP, 1984), the positive inverse contact test indicates that the remanence was acquired before the ~890 Ma sill intrusion. However, this component is approximately antipodal to the HTC of the ~925 Ma sill that intruded the Niyuan Fm. Possible interpretations of this similarity are: (1) the Wangshan Fm is roughly coeval to the sill, and their HTCs represent the dual polarity records of the geomagnetic field around ~925 Ma; (2) the Wangshan Fm is older than this sill but has been remagnetized during intrusion related thermal or fluid event around ~925 Ma; (3) both the Wangshan Fm and this sill were remagnetized at a younger stage. The first two hypotheses both suggest that the HTC is the paleomagnetic records of ~925 Ma. The third hypothesis, however, demands more discussion. The pole derived from the Wangshan Fm (WS, Fig. 12) and the VGP from the ~925 Ma sill (XS1, Fig. 12) fall close to the Late Cambrian and Early Ordovician poles of the NCC (Fig. 12). Some ~520 Ma tectonic events near the southern margin of the NCC have been reported and some authors correlated them with the sedimentary hiatus that existed throughout the NCC between the latest Neoproterozoic and the Epoch 2 of Cambrian (e.g. Han et al., 2009). A remagnetization acquired during this time interval cannot easily be excluded. But the baked contact test between the ~890 Ma sill and the Wangshan Fm strongly suggest that even if such a remagnetization occurred, it must be local. We carried out the sampling in several locations of the Wangshan Fm and the results are same. At the same time, we carried out the sampling of the similar carbonate rocks of the other formations in this region, but we have not found this remanence direction (see discussion in the next paragraph). For these reasons, we interpret the HTCs of the Wangshan Fm and the ~925 Ma sill as the paleomagnetic records of the NCC at ~925 Ma. Of course, there is a fourth hypothesis for the paleomagnetic similarity between the sill "#4" and Wangshan Fm: they could both be primary, and Wangshan Fm is older than 925 Ma, but almost no apparent polar wander (APW) occurred for some amount of time prior to 925 Ma.

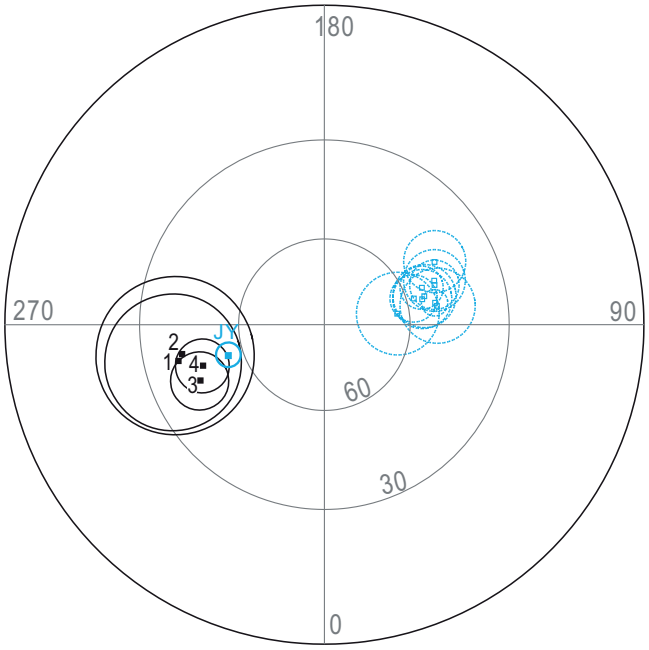

Fig. 13. Paleomagnetic poles derived from the Jiayuan Fm (blue) and those previously published (black) (Fang et al., 1983) from the Jiayuan Fm (1), the Zhaowei Fm (2), the Niyuan Fm (3), the Zhangqu Fm (4). Open/solid square indicates the pole in Northern/Southern hemisphere. Site-mean pole of the Jiayuan Fm (JY) is plotted as its anti-polarity to compare with the previously published poles. (For interpretation of the references to color in this figure legend, the reader is referred to the web version of this article.)

There is no robust field test for the HTC renmanence isolated from the carbonate rocks of the Jiayuan Fm. However, a magnetization carrying an apparently reversed direction from that of the Jiayuan Fm has previously been reported by Fang et al. (1983), although only 26 specimens from eight block samples were studied. Similar directions were also isolated from the Zhaowei, Niyuan and Zhangqu formations (Fang et al., 1983). These four formations occupy the middle part of the Huaibei Group and are all dominated by carbonate rocks. We consider that they may jointly represent a time interval during which the paleomagnetic directions did not change much (Zhang et al., 2000, 2006) but reversals occurred (Fig. 13). We thus further average all site VGPs to get a mean pole for this component (LHB in Fig. 12), which falls at 50.6°S, 107°E ($A_{95} = 3.8°$, Table 6). As this remanence has not been found in the Wangshan Fm or in any other younger rock units in the region, it can be considered to be older than ~925 Ma and younger than the youngest population of detrital zircons (~1120 Ma) of the lower Huaibei Group.

In summary, our new paleomagnetic data include: (1) a new high quality pole for the ~890 Ma mafic sills; (2) a new pole for the Wangshan Fm and the older sill which is likely to be ~925 Ma in age; (3) new data for the middle part of Huaibei Group which were constrained to be between ~925 and ~1120 Ma in age.

5. Implications

5.1. The "Huaibei loop" of apparent polar wander path (APWP) of the NCC

The three poles obtained from the Huaibei Group and the Precambrian sills intruding into it define a new segment of the APWP

Table 6
Paleomagnetic poles used for reconstruction.

Pole	Rock-unit	Age (Ma)	Plat (°N)	Plon (°E)	dp/dm A_{95} (°)	Criterion 1234567 (Q)	Test	References
	Poles from the North China Craton							
XS2	~890 Ma Sills in Huaibei region	890 ± 14, Uz	52.6	330.0	5.3	1111111 (7)	F, C, Rc	This study
XS1	~925 Ma Sill in Huaibei region (VGP)	925 ± 10, Uz	−30.9	136.2	2.4/4.0	1010100 (3)		This study
WS	Wangshan Formation	1121–890, Dz, S	26.1	320.3	5.2	0111100 (4)	F, Cr	This study
NF	Nanfen Formation	<1077, Ud	−16.5	121.1	8.8/13.0	0110101 (4)		Lin (1984), Yang et al. (2012)
LHB	Middle part of Huaibei Group (mean pole)	1121–925, Dz, S	−50.6	107	3.8	0110111 (5)		Fang et al. (1983), Zhang et al. (2000), This study
DJ	Dongjia Formation	1610–520, S	−60.8	97.4	4.3/8.5	0110111 (5)	Rd	Zhang et al. (2000)
	Poles from Baltica							
1	Hunnedalen dykes	848 ± 27, Ar	−41.0	222.0	10/11	1110101 (5)		Walderhaug et al. (1999)
2	Rogaland Ingneous Complex	869 ± 14, Ar	−46.0	238.0	18.1	1110101 (5)		Walderhaug et al. (2007)
3	Egersund-Onga anorthosite	~930,[a] Uz	−42.1	200.4	9.0	0110100 (3)		Brown and McEnroe (2004)
4	Protogine Zone metamorphic, Sweden	950–930,[a] Ar	−45.9	219.4	5.9	0110100 (3)		Pisarevsky and Bylund (1998)
5	Mean ~850 Ma Baltica pole		−43.7	213.3	4.6			Walderhaug et al. (1999)
6	Brattön-Älgö Norite-Anorthosite Complex	916 ± 11, Uz	5.0	249.0	3.9	1110101 (5)		Stearn and Piper (1984), Scherstén et al. (2000)
7	Mean 946–935 Ma Baltica pole	946–935, Ar	−0.9	240.7	6.8	1111111 (7)	C, Rc	Elming et al. (2014)
8	Tärnö-Fäjö dykes	946–954, Ub	12.8	246.7	15.5	1000101 (3)		Patchett and Bylund (1977), Söderlund et al. (2005), Pisarevsky and Bylund (2006)
9	Nilstorp dyke (VGP)	966 ± 2, Ub	9.0	239.0	8.1	1000101 (3)		Patchett and Bylund (1977), Söderlund et al. (2005)
10	Laanila Ristijärvi	1042 ± 50, SN	−2.1	212.2	16.5	0011101 (4)	C	Mertanen et al. (1996)
11	Mean ~1100 Ma Baltica pole		0.7	208.0	16.0			Pesonen et al. (2003)

Dating method of age: Ar = ^{40}Ar–^{39}Ar; Uz = U–Pb zircon; Ub = U–Pb Beddeleyite; Dz = detrital zircon U–Pb age constrained; SN = Sm–Nd; S = stratigraphic correlation. Criterion, the 7-point criterion system of Van der Voo (1990), Q, number of criteria met; Test: F, fold test; C, backed contact test; Cr, inverse contact test; Rc, reversal test (class C of McFadden and McElhinny, 1990). Other abbreviations are the same as in Table 1.

[a] The magnetizations were interpreted as of ~840–870 Ma (Walderhaug et al., 2007; Elming et al., 2014).

for the NCC, a loop with an apex close to the ~925 Ma poles (Fig. 12). Interestingly, two previously reported Precambrian poles also fall on this loop. One is the pole obtained from the Nanfen Fm (NF) in Liaoning Province (Lin, 1984), falling close to the poles of ~925 Ma (Fig. 12). The age of the Nanfen Fm has not been well constrained yet. A recent detrital zircon study (Yang et al., 2012) demonstrated that the Diaoyutai Fm, which is overlain by the Nanfen Fm, is younger than 1077 ± 17 Ma (the youngest age population of the detrital zircons, $n = 6$). The Nanfen Fm is commonly correlated with the lower part of the Huaibei Group (e.g. Xiao et al., 2014), but our paleomagnetic data suggest that the Nanfen Fm should be younger than the lower-middle Huaibei Group and may be close to ~925 Ma in age. Another published pole was obtained from the Dongjia Fm (DJ; Zhang et al., 2000), falling close to the poles from the middle formations of the Huaibei Group (LHB; Fig. 12). The Dongjia Fm is exposed in western Henan Province, also located along the southern margin of the NCC. It contains abundant microfossils (Yin and Guan, 1999), some of which (acritarchs) are also present in the Huaibei Group, suggesting a possible correlation between the Dongjia Fm and the Huaibei Group (Shuhai Xiao, personal communications). However, there is no evidence to confirm which part of the Huaibei Group that can be correlated to the Dongjia Fm. The Dongjia pole may be either older than the Jiayuan pole, or younger than the ~890 Ma pole.

We thus consider this APWP loop to be younger than ~1120 Ma, with an apex close to the 925 Ma poles and an end at the ~890 Ma pole. Most poles of the loop are likely of earliest Neoproterozoic in age, if Xiao et al. (2014)'s analyses are accepted. We herein term this APWP loop, excluding the Dongjia pole at this stage, as the "Huaibei loop".

5.2. Revising the NCC's position in Rodinia

The NCC's position in Rodinia has once been paleomagnetically proposed by Zhang et al. (2006), by matching the coeval APWP segments of the NCC and Laurentia. However, the Precambrian geochronological progress of the NCC (Su et al., 2008, 2010, 2012; Li et al., 2013) demonstrates that most NCC's poles used in that study are significantly older than they were considered to be at that time. The new paleomagnetic and geochronologic results obtained from the Huaibei Group presented here and the sills intruding into these strata allow us to reconsider the reconstruction models.

The "Huaibei loop" has a similar shape and age with the "Sveconorwegian loop" that was recently revised by Elming et al. (2014). If both the NCC and Baltica were part of the supercontinent Rodinia, the two loops should reasonably match. As depicted in Fig. 14, when the NCC is rotated to present Baltica shield using an Euler rotation (72, 87.5, 103.2), to superimpose the ~925 Ma poles of the "Huaibei loop" on top of poles of the similar age poles in the "Sveconorwegian loop", the ~890 Ma pole from the NCC falls on a position between the 870–840 Ma poles and the 960–915 Ma poles of the "Sveconorwegian loop", and NF and the LHB poles fall not so far from the 1100–1000 poles of the "Sveconorwegian loop", This suggests that both NCC and Baltica may be part of a rigid Rodinia during ca. 1100–890 Ma. Since most Grenville poles of the Laurentia are actually older than ~925 Ma (Brown and McEnroe, 2012; Elming et al., 2014), we cannot make a direct comparison between the "Huaibei loop" and the "Grenville loop". However, if we accepted the widely accepted "right-way-up" model (Cawood and Pisarevsky, 2006; Li et al., 2008; Evans, 2009) of the Laurentia–Baltica connection in the Rodinia reconstruction, the NCC would be placed along the arctic Canadian side of the Laurentia (Fig. 14), based on the best

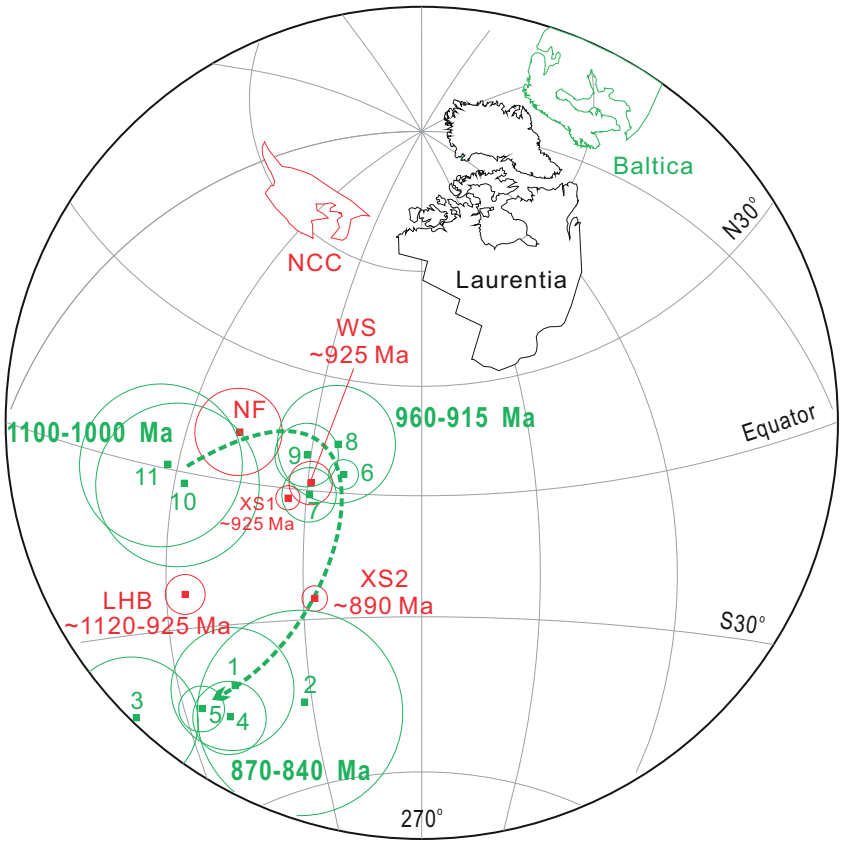

Fig. 14. Possible connection between the NCC and Baltica–Laurentia in Rodinia based on the paleomagnetic data available (all in present northern Europe coordinate). Laurentia is rotated to Baltica according to the "right-way-up" model (Cawood and Pisarevsky, 2006) using Euler rotation (81.5, 250.0, 50.0) (Evans, 2009), the NCC and its poles are rotated to Baltica using Euler rotation (72, 87.5, 103.2). Pole symbols and more information are listed in the Table 6.

fitting between the "Huaibei" and "Sveconorweigian" loops. The gap between the NCC and Baltica is considerablely large in size, implying that the two cratons, if part of the same supercontinent, must have been connected via Greenland and other continental block(s) during the time interval of Rodinia existence (Fig. 14).

A Neoproterozoic proximity between the NCC and São Francisco (SF)–Congo craton has been speculated in recent years based on the new findings of the ~920 Ma large-scale igneous activities in these two cratons (Peng et al., 2011). Our paleomagnetic data obtained from the ~925 Ma sill and Wangshan Fm in the NCC can be directly compared with the paleomagnetic data from the newly dated ~920 Ma dykes exposed in Bahia, Braizil (Evans et al., in press) to test the models of their relationship. The paleomagnetic data of the Bahia dykes suggest a moderate to high paleolatitudinal position of the SF–Congo craton at ~920 Ma, while our ~925 Ma data place the NCC at low latitude. If the NCC at a low latitude neighbored the SF–Congo craton at ~920 Ma as suggested by Peng et al. (2011), their possible connection could be that depicted in Fig. 15b, placing these two cratons in north-south juxtaposition. Furthermore, combined with the "best-fit" model of Huaibei and Sveconorwegian loops, the proximity between the NCC and the SF–Congo can only be permitted if adopting one of the alternative models proposed by Evans et al. (in press), in which the SF–Congo was placed along the present western side of the Laurentia (Fig. 15b). Such a position of SF–Congo, however, faces some geological difficulties, namely that the ~1000 Ma Irumide orogen of SF–Congo has no direct continuation in Laurentia.

Interestingly, our new model also permits that the NCC neighbored Siberia, if the "Laurentia–Siberia" model of Pisarevsky and Natapov (2003) is adopted (Fig. 15). If so, the NCC was located along the present eastern side of the Siberia. Some early Neoproterozoic mafic sills in present southeastern Siberia have been reported (Khudoley et al., 2001; Gladkochub et al., 2010), although they might be tens of million years older than ~920 Ma. If the mafic dykes and sills exposed in Bahia, NCC, southeastern Siberia and Baltica, as well as the relevant volcanic complexes (e.g. reviewed in Peng et al., 2011), have a causal link and represent a large igneous province (LIP) in the earliest Neoproterozoic (Fig. 15b), it should be comparable, in size and latitudinal position, to the LIPs (or plumes) associated with the African Large Low Shear Velocity Province (LLSVP) that was once beneath the Gondwana-land and Pangea (Burke et al., 2008; Torsvik and Cocks, 2013).

The revised NCC's connections in Rodinia still imply its Laurentian proximities, which are supported by the geological evidence listed in the earlier studies (e.g. Li et al., 1996, 2008; Zhang et al., 2000, 2006). However, the NCC's connections in Rodinia suggested here are quite different from its paleomagnetically restructed position in the Nuna supercontinent (e.g. Zhang et al., 2012; Xu et al., 2014; Pisarevsky et al., 2014), indicating that the moved a considerable distance from departing Nuna to joining Rodinia.

5.3. Paleolatitudes of NCC and Rodinia

Our new paleomagnetic data support an equatorial position of the NCC during the time of deposition of the middle part of Huaibei Group carbonates (Fig. 15a). Thereafter the NCC once moved to a slightly higher paleolatitudinal position before ~925 Ma (Fig. 15b), and then moved back to an equatorial position at ~890 Ma (Fig. 15c). Since the number of reliable paleomagnetic poles for the time interval 1100 and 830 Ma is very less, the poles from the Neoproterozoic sills and their host strata of the Huaibei Group provide important paleolatitudinal constraints for the tectonic reconstruction of Rodinia.

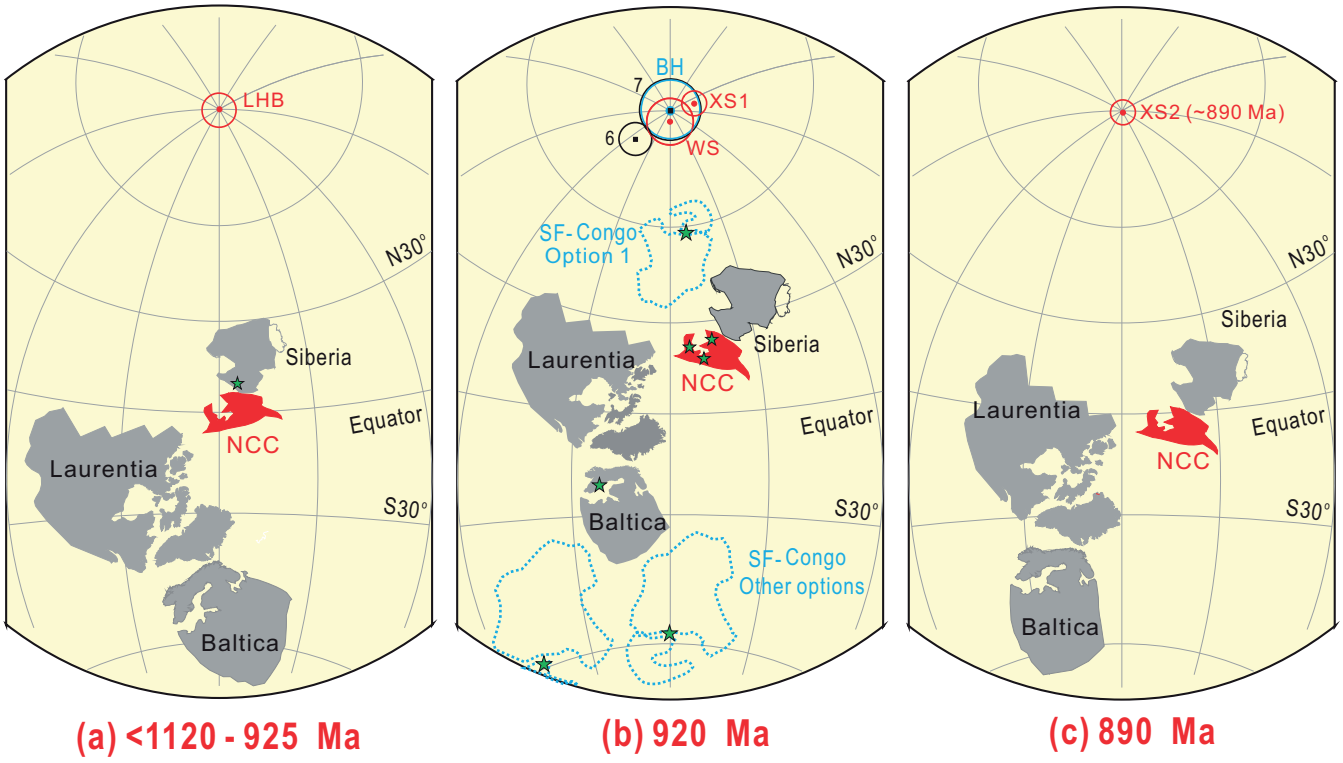

Fig. 15. Paleogeographic positions of the NCC in Rodinia. The NCC–Laurentia–Baltica connection is based on that in Fig. 14. Siberia was rotated to present Laurentia using Euler rotation (65, 144, 141.8) after Pisarevsky and Natapov (2003). Paleomagnetic poles are listed in Table 6. Reconstructions: (a) based on the pole "LHB" from the NCC; (b) position of the NCC–Laurentia–Baltica–Siberia is jointly fixed by using the ~916 Ma (Pole 6 in Table 6) and 935–946 Ma (Pole 7 in Table 6) poles of Baltica, the ~925 Ma poles "WS" and "XS1" of the NCC; paleolatitudinal position of the SF-Congo craton (with different hemisphere options) is determined by using paleomagnetic pole BH (~920 Ma) of the Bahia dyke (Evans, in press), for more details see in text. Green stars showing the ~920 Ma and slightly older mafic dykes and sills discussed in the text; (c) based on the ~890 Ma paleomagnetic pole "XS2" of the NCC. Absolute longitudes for the entire assemblage are arbitrary. The Congo craton was rotated to SF using the Euler rotation (46.8, 329.4, −55.9) after McElhinny et al. (2003). (For interpretation of the references to color in this figure legend, the reader is referred to the web version of this article.)

6. Conclusions

We report a series of paleomagnetic poles obtained from the Huaibei Group and newly dated intrusive sills in the southeastern NCC. The high unblocking temperature component of the ~890 Ma sills passed a baked contact test, a reversal test and a fold test, defining a key pole ($Q = 7$, Van Der Voo, 1990) for the NCC. Even if the quality of the other three poles is lower (see that in Table 6), they are also interpreted as calculated from primary magnetizations. These data together with the poles from the Nanfen Fm and other formations of the middle and lower Huaibei Group depict a loop-like segment of APWP of the NCC, with an apex of ~925 Ma. It is termed the "Huaibei loop" herein.

Comparison between the "Huaibei loop" and the "Sveconorweigian loop", together with the widely accepted "right-way up" model of Laurentia–Baltica connection, suggests the geographic proximities between the NCC and Laurentia in early Neoproterozoic time. The NCC could also be close to the SF–Congo craton around ~925 Ma if the SF–Congo was juxtaposed to the present western side of the Laurentia in Rodinia.

Our data indicate that the NCC was located in a tropic region during probably latest Mesoproterozoic and earliest Neoproterozoic. It moved to a slightly higher paleolatitude by ~925 Ma, and then went back to the equatorial region by ~890 Ma.

Acknowledgements

Authors appreciate the discussions with Profs. Maoyan Zhu, Ganqing Jiang and Shuhai Xiao. We thank Dr. Sergei Pisarevsky, Professor David Evans and an anonymous reviewer for their constructive comments and suggestions that greatly improved this paper. This work was jointly supported by 973 Program (2011CB808800), NSFC Projects 40974035, 40032010B and 40572019. It is a contribution to IGCP 648.

References

BGMRAP (Bureau of Geology and Mineral Resources of Anhui Province), 1987. Regional Geology of Anhui Province. Chinese Ministry of Geology and Mineral Resources, Geological Memoirs, Series 1, Number 5. Geological Publishing House, Beijing, pp. 721.

BGMRJP (Bureau of Geology and Mineral Resources of Jiangsu Province), 1984. Monograph on the regional geology of Jiangsu Province and Shanghai City, People's Republic of China. Chinese Ministry of Geology and Mineral Resources Geological Memoirs, Series 1, Number 1. Geological Publishing House, Beijing, pp. 857.

Brown, L.L., McEnroe, S.A., 2004. Palaeomagnetism of the Egersund–Ogna anorthosite, Rogaland Norway, and the position of Fennoscandia in the late Proterozoic. Geophys. J. Int. 158, 479–488.

Brown, L.L., McEnroe, S.A., 2012. Paleomagnetism and magnetic mineralogy of Grenville metamorphic and igneous rocks, Adirondack Highlands, USA. Precambrian Res. 212–213, 57–74.

Burke, K., Steinberger, B., Torsvik, T.H., Smethurst, M.A., 2008. Plume generation zones at the margins of Large Low Shear Velocity Provinces on the core–mantle boundary. Earth Planet. Sci. Lett. 265, 49–60.

Cao, R., Zhao, W., Xiao, G., 1985. Late Precambrian stromatolites from north Anhui Province. Mem. Nanjing Inst. Geol. Palaeontol. Acad. Sin. 21, 1–54.

Cawood, P.A., Pisarevsky, S.A., 2006. Was Baltica right-way-up or upside-down in the Neoproterozoic? J. Geol. Soc. Lond. 163, 1–7.

Chen, L., Huang, B., Yi, Z., Zhao, J., Yan, Y., 2013. Paleomagnetism of ca 1.35 Ga sills in northern North China Craton and implications for paleogeographic reconstruction of the Mesoproterozoic supercontinent. Precambrian Res. 228, 36–47.

Elming, S.-Å., Pisarevsky, S.A., Layer, P., Bylund, G., 2014. A palaeomagnetic and $^{40}Ar/^{39}Ar$ study of mafic dykes in southern Sweden: a new early Neoproterozoic key-pole for the Baltic shield and implications for Sveconorwegian and Grenville loops. Precambrian Res. 244, 192–206.

Evans, D.A.D., 2009. The palaeomagnetically viable, long-lived and all-inclusive Rodinia supercontinent reconstruction. In: Murphy, J.B., Keppie, J.D., Hynes, A.

(Eds.), Ancient Orogens and Modern Analogues, vol. 327. Geological Society of London Special Publication, pp. 371–404.
Evans, D.A.D., Trindade, R.I.F., Catelani, E.L., D'Agrella-Filho, M.S., Heaman, L.M., Oliveira, E.P., Söderlund, U., Ernst, R.E., Smirnov, A.V., Salminen, J.M., 2015. Return to Rodinia? Moderate to High Palaeolatitude of the São Francisco/Congo Craton at 920 Ma. Geological Society of London Special Publication, 424, http://dx.doi.org/10.1144/SP424.1 (in press).
Fang, D., Guo, Y., Zhu, Z., 1983. Study on the paleomagnetism of upper Precambrian in northern Jiangsu and correlation between the upper Precambrian strata in South and North China. Sci. Geol. Sin. 4, 324–337.
Gao, L., Zhang, C., Liu, P., Tang, F., Song, B., Ding, X., 2009. Reclassification of the Meso- and Neoproterozoic chronostratigraphy of North China by SHRIMP zircon ages. Acta Geol. Sin. 83, 1074–1084 (English edition).
Gladkochub, D.P., Pisarevsky, S.A., Donskaya, T.V., Ernst, R.E., Wingate, M.T.D., Söderlund, U., Mazukabzov, A.M., Sklyarov, E.V., Hamilton, M.A., Hanes, J.A., 2010. Proterozoic mafic magmatism in Siberian craton: an overview and implications for paleocontinental reconstruction. Precambrian Res. 183 (3), 660–668.
Halls, H.C., Li, J., Davis, D., Hou, G., Zhang, B., Qian, X., 2000. A precisely dated Proterozoic palaeomagnetic pole from the North China Craton, and its relevance to palaeocontinental reconstruction. Geophys. J. Int. 143, 185–203.
Han, Y.G., Zhang, S.H., Pirajno, F., Wang, Y., Zhang, Y.H., 2009. New ^{40}Ar–^{39}Ar age constraints on the deformation along the Machaoying fault zone: implications for Early Cambrian tectonism in the North China Craton. Gondwana Res. 16, 255–263.
Huang, B., Zhou, Y., Zhu, R., 2008. Discussions on Phanerozoic evolution and formation of continental China, based on paleomagnetic studies. Earth Sci. Front. 15, 348–359.
Jia, Z., Ning, X., Hong, T., Zheng, W., 2011. The Neoproterozoic molar-tooth carbonate rock veins in northern Anhui and Jiangsu provinces and their forming mechanism. J. Palaeogeogr. 13, 627–634.
Khudoley, A.K., Rainbird, R.H., Stern, R.A., Kropachev, A.P., Heaman, L.M., Zanin, A.M., Podkovyrov, V.N., Belova, V.N., Sukhorukov, V.I., 2001. Sedimentary evolution of the Riphean–Vendian basin of southeastern Siberia. Precamb. Res. 111, 129–163.
Kirschvink, J.L., 1980. The least-squares line and plane and the analysis of palaeomagnetic data. Geophys. J. R. Astron. Soc. 62 (3), 699–718.
Li, Z.X., Zhang, L., Powell, C.M.A., 1996. Positions of the East Asian cratons in the Neoproterozoic supercontinent Rodinia. Aust. J. Earth Sci. 43 (6), 593–604.
Li, H., Lu, S., Su, W., Xiang, Z., Zhou, H., Zhang, Y., 2013. Recent advances in the study of the Mesoproterozoic geochronology in the North China Craton. J. Asian Earth Sci. 72, 216–227.
Li, Z.X., Bogdanova, S.V., Collins, A.S., Davidson, A., De Waele, B., Ernst, R.E., Fitzsimons, I.C.W., Fuck, R.A., Gladkochub, D.P., Jacobs, J., Karlstrom, K.E., Lu, S., Natapov, L.M., Pease, V., Pisarevsky, S.A., Thrane, K., Vernikovsky, V., 2008. Assembly, configuration, and break-up history of Rodinia: a synthesis. Precambrian Res. 160, 179–210.
Lin, J., 1984. The Apparent Polar Wander Paths for the North and South China Blocks. University of California, Santa Barbara, pp. p264.
Liu, Y., Gao, L., Liu, Y., Song, B., Wang, Z., 2006. Zircon U–Pb dating for the earliest Neoproterozoic mafic magmatism in the southern margin of the North China Block. Chin. Sci. Bull. 51, 2375–2382 (English edition).
Liu, Y.Q., Kuang, H.W., Peng, N., Liu, Y.X., Jiang, X.J., Xu, H., 2010. Proterozoic microspar and constraint of sedimentary environment in China. Acta Petrol. Sin. 26, 2122–2130.
Mertanen, S., Pesonen, L.J., Huhma, H., 1996. Palaeomagnetism and Sm–Nd ages of the Neoproterozoic diabase dykes in Laanila and Kautokeino, northern Fennoscandia. In: Brewer, T.S. (Ed.), Precambrian Crustal Evolution in the North Atlantic Region, vol. 112. Geological Society London Special Publication, pp. 331–358.
McFadden, P.L., 1990. A new fold test for paleomagnetic studies. Geophys. J. Int. 103, 163–169.
McFadden, P.L., McElhinny, M.W., 1990. Classification of the reversal test in palaeomagnetism. Geophys. J. Int. 103 (3), 725–729.
McElhinny, M.W., Powell, C.M., Pisarevsky, S.A., 2003. Paleozoic terranes of eastern Australia and the drift history of Gondwana. Tectonophysics 362 (1-4), 41–65.
Meng, X., Ge, M., 2004. The sedimentary features of Proterozoic microspar (molar-tooth) carbonates in China and their significance. Episodes 25, 185–195.
Patchett, P.J., Bylund, G., 1977. Age of Grenville belt magnetization: Rb–Sr and palaeomagnetic evidence from Swedish dolerites. Earth Planet. Sci. Lett. 35, 92–104.
Pei, J., Yang, Z., Zhao, Y., 2006. A Mesoproterozoic paleomagnetic pole from the Yangzhuang Formation. North China and its tectonics implications. Precambrian Res. 151, 1–13.
Peng, P., Bleeker, W., Ernst, R.E., Söderlund, U., McNicoll, V., 2011. U–Pb baddeleyite ages, distribution and geochemistry of 925 Ma mafic dykes and 900 Ma sills in the North China Craton: evidence for a Neoproterozoic mantle plume. Lithos 127, 210–221.
Pesonen, L.J., Elming, S.-Å., Mertanen, S., Pisarevsky, S., D'Agrella-Filho, M.S., Meert, J.G., Schmidt, P.W., Abrahamsen, N., Bylund, G., 2003. Palaeomagnetic configuration of continents during the Proterozoic. Tectonophysics 375, 289–324.
Pisarevsky, S.A., Bylund, G., 1998. Palaeomagnetism of a key section of the Protogine Zone, southern Sweden. Geophys. J. Int. 133, 185–200.
Pisarevsky, S.A., Bylund, G., 2006. Palaeomagnetism of 935 Ma mafic dykes in southern Sweden and implications for the Sveconorwegian Loop. Geophys. J. Int. 166, 1095–1104.
Pisarevsky, S.A., Natapov, L.M., 2003. Siberia and Rodinia. Tectonophysics 375, 221–245.
Pisarevsky, S.A., Elming, S.-Å., Pesonen, L.J., Li, Z.-X., 2014. Mesoproterozoic paleogeography: supercontinent and beyond. Precambrian Res. 244, 207–225.
Ren, Q., Zhang, S., Li, H., Wu, H., Yang, T., Liang, Z., Miao, X., Zhao, H., 2015. Further paleomagnetic results from the ~155 Ma Tiaojishan Formation, North China, and their tectonic implications. Gondwana Res., http://dx.doi.org/10.1016/j.gr.2015.05.002.
Scherstén, A., Årebäck, H., Cornell, D., Hoskin, P., Åberg, A., Armstrong, R., 2000. Dating mafic–ultramafic intrusions by ion-microprobing contact melt zircon: examples from SW Sweden. Contrib. Mineral. Petrol. 139, 115–125.
Söderlund, U., Isachsen, C.E., Bylund, G., Heaman, L., Patchett, P.J., Vervoort, J.D., Andersson, U.B., 2005. U–Pb baddeleyite ages and Hf Nd isotope chemistry constraining repeated mafic magmatism in the Fennoscandian shield from 1.6 to 0.9 Ga. Contrib. Mineral. Petrol. 150, 174–194.
Stearn, J.E.F., Piper, J.D.A., 1984. Palaeomagnetism of the Sveconorwegian mobile belt of the Fennoscandian shield. Precambrian Res. 23, 201–246.
Su, W., Li, H., Huff, W., Ettensohn, F., Zhang, S., Zhou, H., Wan, Y., 2010. SHRIMP U–Pb dating for a K-bentonite bed in the Tieling Formation, North China. Chin. Sci. Bull. 55, 3312–3323.
Su, W.-B., Li, H.-K., Xu, L., Jia, S.-H., Geng, J.-Z., Zhou, H.-Y., Wang, Z.-H., Pu, H.-Y., 2012. Luoyu and Ruyang Group at the south margin of the North China Craton (NCC) should belong in the Mesoproterozoic Changchengian System: direct constraints from the LA-MC-ICPMS U–Pb age of the tuffite in the Luoyukou Formation, Ruzhou, Henan, China. Geol. Surv. Res. 35 (2), 96–108 (in Chinese with English abstract).
Su, W., Zhang, S., Huff, W.D., Li, H., Ettensohn, F.R., Chen, X., Yang, H., Han, Y., Song, B., Santosh, M., 2008. SHRIMP U–Pb ages of K-bentonite beds in the Xiamaling Formation: implications for revised subdivision of the Meso- to Neoproter- ozoic history of the North China Craton. Gondwana Res. 14, 543–553.
Torsvik, T.H., Cocks, L.R.M., 2013. Gondwana from top to base in space and time. Gondwana Res. 24, 999–1030.
Van der Voo, R., 1990. The reliability of paleomagnetic data. Tectonophysics 184, 1–9.
Walderhaug, H.J., Torsvik, T.H., Eide, E.A., Sundvoll, B., Bingen, B., 1999. Geochronology and palaeomagnetism of the Hunnedalen dykes. SW Norway: implications for the Sveconorwegian apparent polar wander loop. Earth Planet. Sci. Lett. 169, 71–83.
Walderhaug, H.J., Torsvik, T.H., Halvorsen, E., 2007. The Egersund dykes (SW Norway): a robust Early Ediacaran (Vendian) palaeomagnetic pole from Baltica. Geophys. J. Int. 168, 935–948.
Wang, H., Zhang, S., He, G., 2005. China and Mongolia. In: Richard, C.S., Cocks, L.R.M., Plimer, I.R. (Eds.), Encyclopedia of Geology. Elsevier, Oxford, pp. 345–357.
Wang, Q., Yang, D., Xu, W., 2012. Neoproterozoic basic magmatism in the southeastmargin of North China Craton: evidence from whole-rock geochemistry U–Pb and Hf isotopic study of zircons from diabase swarms in the Xuzhou–Huaibeiarea of China. Sci. Chin. Earth Sci. 55, 1461–1479.
Watson, G.S., Enkin, R.J., 1993. The fold test in paleomagnetism as a parameter estimation problem. Geophys. Res. Lett. 20, 2135–2137.
Wu, H., Zhang, S., Li, Z.X., Li, H., Dong, J., 2005. New paleomagnetic results from the Yangzhuang Formation of the Jixian System. North China, and tectonic implications. Chin. Sci. Bull. 50, 1483–1489.
Xiao, S., Shen, B., Tang, Q., Kaufman, A.J., Yuan, X., Li, J., Qian, M., 2014. Biostratigraphic and chemostratigraphic constraints on the age of early Neoproterozoic carbonate successions in North China. Precambrian Res. 246, 208–225.
Xing, Y., 1989. The Upper Precambrian of China, Stratigraphy of China, No. 3. Geological Publishing House, Beijing, pp. 1–314 (in Chinese).
Xu, H., Yang, Z., Peng, P., Meert, J.G., Zhu, R., 2014. Paleo-position of the North China Craton within the supercontinent Columbia: constraints from new paleomagnetic results. Precambrian Res. 255, 276–293.
Yang, D.-B., Xu, W.-L., Xu, Y.-G., Wang, Q.-H., Pei, F.-P., Wang, F., 2012. U–Pb ages and Hf isotope data from detrital zircons in the Neoproterozoic sandstones of northern Jiangsu and southern Liaoning Provinces. China: implications for the late Precambrian evolution of the southeastern North China Craton. Precambrian Res. 216-219, 162–176.
Yin, L., Guan, B., 1999. Organic-walled microfossils of Neoproterozoic Dongjia Formation, Lushan County, Henan Province North China. Precambrian Res. 94, 121–137.
Zhang, S., Li, Z., Evans, D.A.D., Wu, H., Li, H., Dong, J., 2012. Pre-Rodinia supercontinent Nuna shaping up: a global synthesis with new paleomagnetic results from North China. Earth Planet. Sci. Lett. 353–354, 145–155.
Zhang, S., Li, Z., Wu, H., 2006. New Precambrian paleomagnetic constraints on the position of the North China Block in Rodinia. Precambrian Res. 144 (3-4), 213–238.
Zhang, S., Li, Z., Wu, H., Wang, H., 2000. New paleomagnetic results from the Neoproterozoic successions in southern North Block and paleogeographic implications. Sci. Chin. D 43 (Suppl.), 233–244.
Zhu, M., 2010. The origin and Cambrian explosion of animals: fossil evidence from China. Acta Palaeontol. Sin. 49 (3), 269–287.